AEDC-TR-70-64

M9

ABLATION TESTING IN HOT AND COLD COAXIAL JETS - PHASE I, COLD FLOW FEASIBILITY TESTS

R. D. Herron
ARO, Inc.

April 1970

PROPULSION WIND TUNNEL FACILITY
ARNOLD ENGINEERING DEVELOPMENT CENTER
AIR FORCE SYSTEMS COMMAND
ARNOLD AIR FORCE STATION, TENNESSEE

NOTICES

When U. S. Government drawings specifications, or other data are used for any purpose other than a definitely related Government procurement operation, the Government thereby incurs no responsibility nor any obligation whatsoever, and the fact that the Government may have formulated, furnished, or in any way supplied the said drawings, specifications, or other data, is not to be regarded by implication or otherwise, or in any manner licensing the holder or any other person or corporation, or conveying any rights or permission to manufacture, use, or sell any patented invention that may in any way be related thereto.

Qualified users may obtain copies of this report from the Defense Documentation Center.

References to named commercial products in this report are not to be considered in any sense as an endorsement of the product by the United States Air Force or the Government.

ABLATION TESTING IN HOT AND COLD COAXIAL JETS - PHASE I, COLD FLOW FEASIBILITY TESTS

R. D. Herron
ARO, Inc.

FOREWORD

The research reported herein was sponsored by the Arnold Engineering Development Center (AEDC), Air Force Systems Command (AFSC), under Program Element 62201F, Project 8950, Task 12.

The results of research presented in this report were obtained by ARO, Inc. (a subsidiary of Sverdrup & Parcel and Associates, Inc.), contract operator of the AEDC, AFSC, Arnold Air Force Station, Tennessee, under Contract F40600-69-C-0001. The work was performed from July 1968 to November 1969 under ARO Projects PW5903 and PW5003, and the manuscript was submitted for publication on February 2, 1970.

This technical report has been reviewed and is approved.

David C. Reynolds
1st Lt, USAF
Research Division
Directorate of Plans
and Technology

Harry L. Maynard
Colonel, USAF
Director of Plans
and Technology

ABSTRACT

An investigation was conducted to determine the feasibility of extending the capability of ablation test facilities by surrounding the high enthalpy flow with a coaxial cold air jet. The investigation included both analytical and cold flow experimental studies. It was determined that the coaxial flow technique is extremely promising, offering the potential of easily doubling the facility model size capability. Results of the cold flow experimental tests and criteria for application of the technique to high enthalpy facilities are presented.

CONTENTS

APPENDIX
ILLUSTRATIONS

Figure

NOMENCLATURE

C_p	Pressure coefficient, $\left(\frac{p}{p_H} - 1\right) / \frac{\gamma}{2} M^2$
$C_{p_{max}}$	Stagnation point pressure coefficient, $\left(\frac{p_{t_2}}{p_H} - 1\right) / \frac{\gamma}{2} M^2$
M	Mach number
p	Flow static pressure or probe or model pressure
p_t	Total pressure
p_{t_2}	Pitot pressure
p_∞	Ambient or test cell pressure
r	Radial distance normal to jet centerline
r_e	Nominal central nozzle exit radius, 0.5 in.
r_n	Reentry model nose radius, 0.72 in.
s	Distance measured from the nose along the reentry model surface
T_t	Stagnation temperature measured by the traversing probe
T_{t_H}	Central stream total temperature
U	Flow velocity
x	Distance from the central nozzle exit measured along the nozzle axis, positive downstream

x_m	Distance from the tip of the 10-deg cone model measured along the model axis, positive downstream from the tip
γ	Ratio of specific heats
δ	Flow deflection angle, see Eq. (1)
θ	Angle between the flow axis and a line normal to the model surface

SUBSCRIPTS

c	Cold air or annular flow conditions
H	High enthalpy or central flow conditions

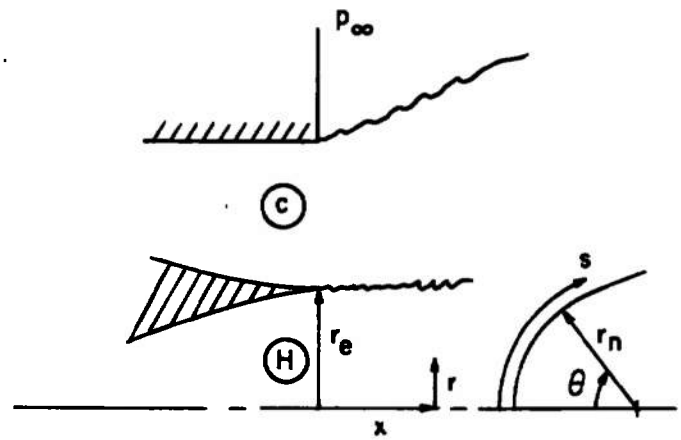

SECTION I
INTRODUCTION

The requirement for studying ablation and other phenomena associated with very high-speed flight has led to the development of a variety of small, high enthalpy, high pressure test facilities. The very large power requirements as well as problems encountered in developing large or multiple-arc heaters have limited the size of these facilities. Since the facility is operated at high stagnation pressures and exhausts to atmospheric pressure, a nonuniform expanding flow field exists over much of the model nose, beginning with the intersection of the nozzle Mach wave with the model, as shown in Fig. 1a, Appendix. Therefore, for nose cone ablation tests of the types recently conducted, only a limited region of uniform flow is obtained. One method of eliminating the expansion would be to place the facility and the model in a pressurized tank. However, this presents many serious operational and hardware problems.

Another method, as discussed herein, is to surround the high enthalpy flow with a coaxial cold air jet with static pressures matched at the interface. The coaxial jet will eliminate the expansion at the high enthalpy nozzle exit, thereby providing the correct flow field over a much larger region of the model. This is typically shown in Fig. 1b. Also for ablation testing of blunt bodies, a proper matching of the cold airflow would impose the correct flow field over a body very large relative to the high enthalpy flow nozzle. Valid ablation data could then be obtained until the mixing of the flows finally reduces the enthalpy of the model boundary layer. This coaxial flow technique would therefore improve the quality of the flow field, permit the testing of larger models, or reduce the facility power requirements.

The objective of the investigation reported herein was to determine the feasibility of the concept and to develop the required criteria for applying the technique to high enthalpy test facilities. The investigation included both analytical and cold flow experimental studies.

SECTION II
PROBLEM AREAS AND ANALYTICAL CONSIDERATIONS

In the development of the coaxial flow concept, three major problem areas arise. They are (1) the aerodynamic interaction of the two flows with the model, (2) the very real hardware problems arising in applying

the technique to a high enthalpy facility, and (3) the viscous mixing between the flows. The problems will be discussed further in this section.

2.1 AERODYNAMIC INTERACTIONS

Problems with the aerodynamic interaction of the two flows arise not only in developing and bringing the two flows together without major disturbances, but also in determining criteria for "tailoring" the flows to obtain a satisfactory aerodynamic flow field on the test model. To eliminate a shock and expansion at the junction of the flows will require the flows to have equal static pressures at the nozzle exits. But even if equal pressure, inviscid, uniform flow from each of the nozzles and a zero-thickness nozzle wall could be obtained, the coaxial flow interaction with the model flow field must still be considered since the two flows will have different gas specific heat ratios.

2.1.1 Slender Bodies

For slender bodies, the primary benefit to be obtained from the coaxial cold air jet is to move the flow expansion to atmospheric pressure from the high enthalpy nozzle exit to the outer cold air nozzle exit. Therefore, depending upon the relative size of the jets, a significantly larger region of the model may be tested.

However, a problem arises in that at the intersection of the model shock and the high enthalpy jet boundary, a reflected shock or expansion must occur unless the pressure change and the angle change for the two flows are exactly matched behind the model shock. This is shown below in the sketch of an idealized flow field.

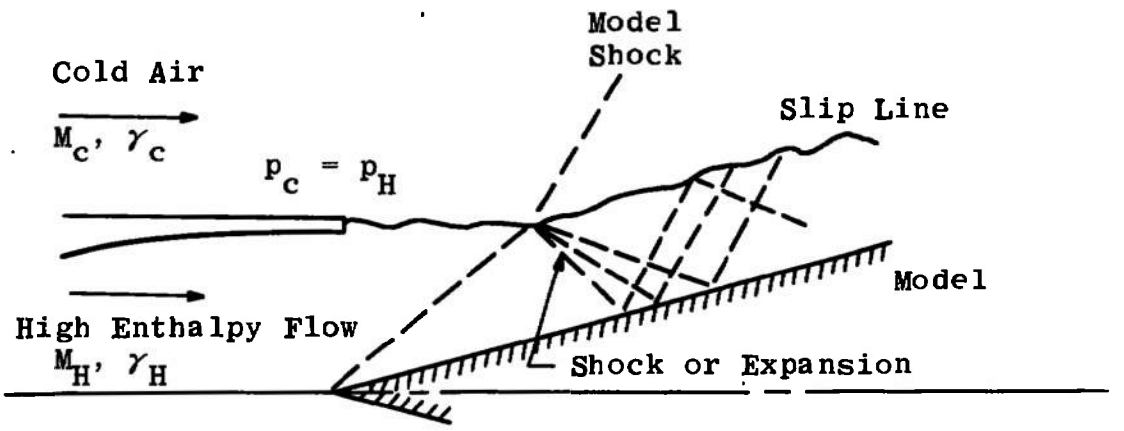

For two-dimensional expansions or compressions (which must also be valid locally at the slip line-shock intersection) through small angles the following relation holds:

$$\frac{\Delta p}{p} = \pm \frac{\gamma M^2}{\sqrt{M^2-1}} \Delta\delta + \gamma M^2 \frac{(\gamma+1)M^4 - 4(M^2-1)}{4(M^2-1)^2} (\Delta\delta)^2 \qquad (1)$$

$$\pm \text{ higher order terms}$$

Therefore, for small slender bodies a matching of the linearized relation for $\Delta p/\Delta\delta$ will approximate the desired matching near the slip line-shock intersection. This requires a "tailoring" of the two flows such that

$$\left.\frac{\gamma M^2}{\sqrt{M^2-1}}\right)_{\substack{\text{cold}\\ \text{air}\\ \text{jet}}} = \left.\frac{\gamma M^2}{\sqrt{M^2-1}}\right)_{\substack{\text{high}\\ \text{enthalpy}\\ \text{jet}}} \qquad (2)$$

in addition to the requirement for equal static pressure at the nozzle exits.

2.1.2 Large Blunt Bodies

The criteria of Eq. (2) would not be expected to give satisfactory results for large blunt bodies where large flow deflections are required. However, if the correct model pressure distribution can be obtained, and the dividing streamline between the cold and the high enthalpy gas still be located outside the model boundary layer, the correct test conditions at the model surface will result. The exception would be cases where gas radiation contributes a significant heat load to the aft regions of the model. As will be shown later, the modified Newtonian theory gives a good representation of the pressure distribution over the nose region of blunt bodies. This relation is

$$\frac{C_p}{C_{p_{max}}} = \cos^2 \theta \qquad (3)$$

Applying this relation on each side of the dividing streamline between the two flows as the flows approach the model shock (coincident with the body for Newtonian theory) establishes the requirement

$$\left.\frac{C_p}{C_{p_{max}}}\right)_{\substack{\text{cold}\\ \text{air}\\ \text{jet}}} = \left.\frac{C_p}{C_{p_{max}}}\right)_{\substack{\text{high}\\ \text{enthalpy}\\ \text{jet}}} \qquad (4)$$

but since the static pressures of the two flows are equal and the body surface pressure must be equal on each side of the dividing streamline, the criterion is established that the pitot pressure of the two jets be equal.

The required Mach number relation for the flows may be obtained from the Rayleigh pitot formula:

$$\frac{p_{t_2}}{p} = \left[\frac{(\gamma+1)M^2}{2}\right]^{\frac{\gamma}{\gamma-1}} \left[\frac{\gamma+1}{2\gamma M^2 - (\gamma-1)}\right]^{\frac{1}{\gamma-1}} \tag{5}$$

However, in practice, the desired relationship may be readily obtained from flow tables corresponding to the specific heat ratios of the two jets. Restating, the criteria for coaxial flows over large blunt bodies are

$$p)_{\substack{\text{cold}\\\text{air}\\\text{jet}}} = p)_{\substack{\text{high}\\\text{enthalpy}\\\text{jet}}} \tag{6}$$

and

$$\frac{p_{t_2}}{p}\Big)_{\substack{\text{cold}\\\text{air}\\\text{jet}}} = \frac{p_{t_2}}{p}\Big)_{\substack{\text{high}\\\text{enthalpy}\\\text{jet}}} \tag{7}$$

It should be noted that the different criteria given for slender and for blunt bodies fortunately do not result in drastically different Mach numbers for the cold airflows, at least for high enthalpy flows with Mach numbers of interest for ablation testing. Also, both sets of criteria result in a lower Mach number for the cold airflow than for the high enthalpy flow. This requires a lower total pressure and a lower mass flow for the cold air than would be required if the Mach number of the two flows was equal.

2.2 HARDWARE CONSIDERATIONS

During this investigation studies were made of the problems arising in designing, fabricating, and operating the coaxial flow hardware. In these studies, two major problems become obvious. These are the very small size of the high enthalpy flow nozzle and the necessity for cooling the surfaces exposed to the high enthalpy flow.

Ideally, the hardware should develop coaxial uniform flows with no disturbances generated by bringing the flows together. Obviously, this

cannot be accomplished. The finite thickness at the nozzle exit causes a flow expansion and compression analogous to the flow over a backward facing step. This step becomes physically more significant as the size of the hardware is decreased. The design of the nozzles should bring the flows together at as small and as near equal angles as possible. However, in order to water cool as much of this nozzle lip as possible, the nozzle must have a large wall angle. Also, the high enthalpy flow nozzle should be short to minimize the heat transferred to the nozzle. Fortunately, for the testing of blunt bodies, even large flow disturbances at the nozzle exit are weak when compared with the blunt-body shock.

Figure 2 shows a preliminary design for an arc-heater application. The lack of space between the nozzles for water cooling is evident. Water cooling for all of the lip between the nozzles is not possible. However, some backside cooling is obtained from the cold airflow and some axial cooling to the water passage will be obtained. These considerations place some lower limit on the Mach number and on the physical size of the high enthalpy flow. The design studies do show that hardware can be fabricated for an arc heater with a nozzle throat as small as 3/8 in. in diameter and an exit Mach number of 2.5. Nearly all of the problems discussed become more tractable as the size of the hardware is increased. In particular, increasing the size of the nozzle for the high enthalpy flow and a careful design optimization should permit a larger annular aiflow and/or a lower Mach number for the high enthalpy flow. A lower Mach number for the high enthalpy flow would be desirable where a very high model stagnation pressure is required.

2.3 VISCOUS MIXING ALONG THE DIVIDING STREAMLINE

Even if the correct aerodynamic matching is obtained, viscous mixing of the two flows will invalidate the flow field at some point downstream on the model. Much effort has been directed by many investigators to the problem of two-stream mixing. However, the present problem is that of the mixing of compressible, nonisoenergetic, three-dimensional streams of different gases with initially disturbed flow profiles, and therefore a most difficult problem to handle analytically. In addition, the influence of the model shock system on the mixing process is not known.

Current analytical techniques have been studied and an estimate made of the mixing process for high enthalpy, coaxial flow applications. The method used was an integral technique developed by Korst (Ref. 1) for compressible two-stream mixing with a Prandtl number of one. Estimates by Lamb (Ref. 2) were used for the effects of nonisoenergetic

mixing on the required similarity parameter. Results of a sample calculation are shown in Fig. 3 for different values of the velocity ratio between the two streams. It should be noted that (1) the spread of the velocity mixing region in the high enthalpy flow is not large, and (2) the cold airflow does reduce the spread of the mixing region into the high enthalpy flow.

This relatively small rate of growth of the mixing region makes the coaxial technique appear feasible; however, it lacks experimentally verified values for the similarity parameter which governs the spread rate. Therefore, unpublished experimental pitot pressure surveys obtained in an arc heater were analyzed. These surveys were compared with the theoretical calculations for the case of single-stream mixing and the results are shown in Fig. 4. The quite good agreement between theory and experiment gives some confidence in the theoretical calculations and in the values chosen for the similarity parameter. In general, it does not appear that the viscous mixing will invalidate model ablation data until well back on the test model.

SECTION III
COLD FLOW TEST APPARATUS

To verify the coaxial flow concept and to provide further insight into problems to be encountered in applying the concept, cold flow experimental tests were conducted. Cold flow tests were chosen partially because of the relatively high costs of high enthalpy flow experiments, but especially because of the extreme difficulty in obtaining significant measurements in a high enthalpy flow. These tests were conducted in the Propulsion Wind Tunnel (PWT) 1-ft Aerodynamic Wind Tunnel (1S) modified to be used as an evacuated test chamber.

The configurations of the coaxial flow nozzle assembly and the reentry-type model used in these cold flow tests are shown in Fig. 5 and the installation is shown in Fig. 6. The central stream is carbon dioxide gas heated to approximately 800°R and with a nominal exit Mach number of 2.5. Carbon dioxide gas (CO_2) was chosen to simulate the high enthalpy flow because its specific heat ratio is representative of such flows. All calculations for the carbon dioxide flow assumed a perfect gas with a specific heat ratio of 1.28. The annular air jet was unheated air at a stagnation temperature of approximately 480°R. Two different annular nozzles were used to give the air jet a nominal exit Mach number of either 2.0 or 2.5. The carbon dioxide total pressure was nominally 50 psia with the air stagnation pressure usually set to

give equal static pressure at the nozzle exits. The test chamber could be evacuated to permit operation at an ambient pressure as low as 70 psfa, thereby simulating the expanding flow field of a high pressure-high enthalpy facility exhausting to atmosphere. The ambient pressure could also be set equal to the nozzle exit static pressure, thereby simulating the proposed operation of high enthalpy facilities in a pressurized tank.

Prior to designing the cold flow nozzle assembly, a preliminary design (Fig. 2) was made for application of the coaxial flow concept to a Linde 5-MW, N-4000 arc heater with a 3/8-in. throat diameter nozzle. The nozzles for the cold flow tests were then designed to be consistent with space and configuration limitations of the high enthalpy application. The size of the air jet relative to the high enthalpy jet is not the maximum that could be obtained, but was selected to be compatible with the different air jet nozzles required by the different flow matching criteria. Once criteria for the two flows have been established, a careful design optimization for a particular facility should permit some increase in the air jet size. The nozzles for the cold flow tests are shorter than would be desired to develop uniform, parallel flow but are typical of a high enthalpy facility application. Both the central CO_2 and the annular air nozzles were designed by computer programs utilizing the method of characteristics. No corrections were made for the nozzle boundary layer. The configuration and the design coordinates for the nozzles are shown in Fig. 7. Because of a fabrication error, the dimensions of the CO_2 nozzle differ substantially from the design values and therefore a set of "as built" coordinates are also presented.

Two pressure-instrumented models were used in the cold flow tests. One was a sharp 10-deg cone model and the other a large hemisphere 10-deg cone, reentry shape model. Both models have a 2-in. base diameter. The reentry shape model has a nose radius of 0.72 in., which is the equivalent of a 1/2-in. nose radius model when the cold flow nozzle assembly is scaled to that typical of the 3/8-in. throat diameter, 5-MW arc heater. Normally models no larger than 1/4-in. radius are tested in these arc heaters. Both models were tested at varying axial positions as well as both with and without the annular cold airflow. Model pressures were measured on a mercury manometer and recorded photographically. An error analysis based on a 95-percent confidence level shows the pressure data presented to be accurate to $p/p_{t_2} = \pm 0.006$ for the reentry body data and to $p/p_t = \pm 0.005$ for the 10-deg cone data.

In addition to the pressure models, pitot pressure and total temperature surveys were made of the nozzle flow field without the models present. Also, schlieren photographs of the flow field were taken both with and without models present.

SECTION IV
EXPERIMENTAL RESULTS AND DISCUSSION

4.1 COAXIAL FLOW FIELDS

Prior to the model tests, pitot pressure and stagnation temperature surveys were made through the coaxial flow fields. The results of these surveys are shown in Figs. 8 and 9 for conditions where the ambient or cell pressure is equal to the nozzle exit static pressure. Schlieren photographs of the corresponding flows are shown in Fig. 10. These data show the two streams to be of a generally good quality with nominally the design Mach numbers. Both the pitot pressure and the stagnation temperature distributions show very sharp boundaries between the hot CO_2 and the cold airflow. There is very little momentum or energy mixing between the two flows, which is in agreement with predictions for flows with nearly equal velocities.

Although the stagnation temperature distributions are very uniform, the pitot pressure uniformity is poorer than hoped for. The nozzles were of an arc-heater-type design, being short to minimize nozzle heat transfer. The short design and the manufacturing inaccuracies previously discussed resulted in the CO_2 stream having a nonuniform flow, particularly along the nozzle axis. The axisymmetric design may provide a "focusing" of wall disturbances on the nozzle centerline. This centerline nonuniformity also becomes evident in the model stagnation point pressure data. Shown in Fig. 11 is a compilation of pitot probe and reentry model stagnation pressure data which emphasizes the axial variation. The model stagnation pressure data shown have been shifted upstream by $0.16\ r_e$, which is the theoretical model shock stand-off distance. Model data are shown both with and without the coaxial airflow. Also shown is the pressure near the nozzle exit as calculated by a method-of-characteristics solution for the "as built" nozzle contour. These data show the centerline disturbance to be caused by the central nozzle and not by the coaxial airflow. Although the centerline flow is not as uniform as desired, it is generally as good as that obtained in arc-heated flows from contoured nozzles, particularly after nozzle erosion has occurred.

4.2 REENTRY-TYPE MODEL TESTS

To evaluate the results of the model tests, an experimental or theoretical basis of comparison is needed. Several wind tunnel studies of reentry bodies have shown the modified Newtonian theory to give very good results from the nose to near the junction of the sphere and the cone. Figure 12 shows a comparison of this theory with wind tunnel data from Ref. 3 for conditions very near those of the current tests. Also shown are the theoretical values from Refs. 4 and 5 for 10-deg cones, which the experimental data should approach asymptotically. The subsequent figures presenting the coaxial flow data will show the theory (corrected for $\gamma = 1.28$) as a basis for comparison. Because of the nonuniform flow on the nozzle centerline, the coaxial flow data are ratioed to the pitot pressure for uniform flow with a specific heat ratio of 1.28 and a Mach number of 2.5 instead of the measured stagnation point pressure.

The results of tests without the annular air jet are shown in Fig. 13. For such a large model, the pressure rapidly falls off to the ambient pressure, providing a very limited region of useful data. Schlieren photographs corresponding to these data are shown in Fig. 14. One proposal for increasing the flow quality and the model size capability of present arc heaters has been to place the arc heater and the model in a pressurized tank. As shown in Fig. 15, such a technique would provide only a small improvement for such a large model.

The previous theoretical analysis based on the modified Newtonian theory (Section 2.1.2) has shown that the matching of the static and the pitot pressures would be required for large blunt bodies, therefore requiring an airflow Mach number of 2.42 for the cold flow tests. Results of the tests with the annular airflow having the "incorrect" Mach number of 2.0 are shown in Fig. 16. A significant improvement is seen over the data previously presented without the air jet. However, as expected from the theory, the pressures are too low over the region of the model that is influenced by the annular air jet.

When the air jet Mach number is changed to 2.5, close to the required 2.42, a remarkable improvement is found. The results of tests at an axial position typical of ablation testing are shown in Figs. 17 and 18. The annular air jet provides the desired flow past the sphere-cone junction of a model that is twice the size that can normally be tested. The technique therefore offers the potential of at least doubling the model size capability of high enthalpy facilities. Although it was not evaluated in these tests, the coaxial technique should give valid data even further aft on relatively smaller models. The decrease in pressure

aft of the junction is caused by the expanding flow field originating at the air nozzle outer lip, which would be eliminated in a pressurized tank. The results of tests simulating the tank, given in Figs. 19 and 20, show that the desired flow field can be obtained even further back on this large model. The results of the reentry model tests therefore show that the flow matching criteria based on the modified Newtonian theory (Section 2.1.2) to be correct for large blunt bodies.

The results of tests to determine the effect of model position are shown in Figs. 21 and 22. Two effects are noted: (1) As expected, with the model very far downstream ($x/r_e = 5$) the expansion from the outer lip of the air nozzle strikes most of the model causing the model pressures to be too low. (2) When the model is very close ($x/r_e \leq 1/2$) the rise in pressure from the model shock propagates through the mixing region and causes a separation of the flow fields. This is noted in the pressure dip at $s/r_n \approx 0.8$ for the data at $x/r_e = 1/2$. However, neither of the phenomena is considered to be a problem in the actual application of the technique.

4.3 CONE MODEL TESTS

Tests were also conducted with a 10-deg cone model to establish criteria for the testing of small, slender bodies in coaxial flows. As discussed in Section 2.1.1, the primary benefit expected from the coaxial jet is to move the flow expansion downstream on the model and thereby provide a significantly larger test region on the model. That this result is in fact achieved is shown in Fig. 23. These results show the annular air jet to increase the valid test region axially on the model from approximately one nozzle exit radii to from three to four radii. Also, larger increases would be obtained by relatively larger annular air nozzles. The theoretical pressure ratio shown is from Refs. 4 and 5, corrected for a specific heat ratio of 1.28. The deviations about the theoretical value are believed to be caused primarily by the non-uniform central nozzle flow and perhaps to a lesser extent by the incorrect Mach numbers of the annular air jets. An air jet Mach number of 2.25 would be required to match the slender body criteria given in Section 2.1.1. However, as shown by Fig. 23a, a facility designed by the blunt-body criteria could well be used to test slender bodies also.

The effect of the coaxial air jet for simulated tests in a pressurized tank is shown in Fig. 24. The coaxial jet provides an improvement in the model flow field by reducing the model shock-jet boundary interaction, but the improvements are not as pronounced as shown for the tests simulating an atmospheric exhaust.

SECTION V
CONCLUDING REMARKS

The analytical and cold flow experimental investigation of ablation testing in the flow field of coaxial hot and cold jets indicates the following conclusions:

1. The coaxial flow technique will provide the correct flow field over the nose region of relatively very large, reentry-type models and the technique can substantially increase the facility model size capability.

2. For very slender bodies, the coaxial technique can increase the model length for which valid data can be obtained by a factor of at least two to four. This is achieved primarily by moving the flow expansion to atmospheric pressure from the high enthalpy nozzle to the cold air nozzle exit.

3. The flow matching criteria based on the modified Newtonian theory is valid for large reentry-type models. A facility designed for the reentry body criteria can well be used for slender bodies also.

4. Although the small physical size and the requirement for cooling the high enthalpy nozzle present significant design problems, the studies show that hardware can be fabricated for a 5-MW arc heater with a nozzle throat as small as 3/8-in. in diameter and an exit Mach number of 2.5.

5. It does not appear that viscous mixing between the flows will invalidate the data for currently envisioned tests until well back on the test models. However, experimentally verified data for this type of mixing process is needed.

6. The concept of testing in a pressurized tank (hot flow only) will not provide a significant improvement in capability for large, blunt models as used in this investigation. The pressurized tank does provide an improvement in capability when used with the coaxial flow technique.

REFERENCES

1. Korst, H. H. and Chow, W. L. "Non-Isoenergetic Turbulent (Pr_t = 1) Jet Mixing between Two Compressible Streams at Constant Pressure." NASA CR-419, April 1966.

2. Lamb, J. P. "An Approximate Theory for Developing Turbulent Free Shear Layers." Journal of Basic Engineering, September 1967, p. 633.

3. Sawyer, Wallace C. and Smith, Rudeen S. "Experimental Surface-Pressure Distributions on a 9° Spherically Blunted Cone at Mach Numbers from 1.50 to 4.63." NASA TM X-1730, January 1969.

4. Staff of the Computing Section. Tables of Supersonic Flow around Cones. Massachusetts Institute of Technology, Department of Electrical Engineering, 1947.

5. Sims, Joseph L. "Tables for Supersonic Flow around Right Circular Cones at Zero Angle of Attack." NASA SP-3004, 1964.

APPENDIX
ILLUSTRATIONS

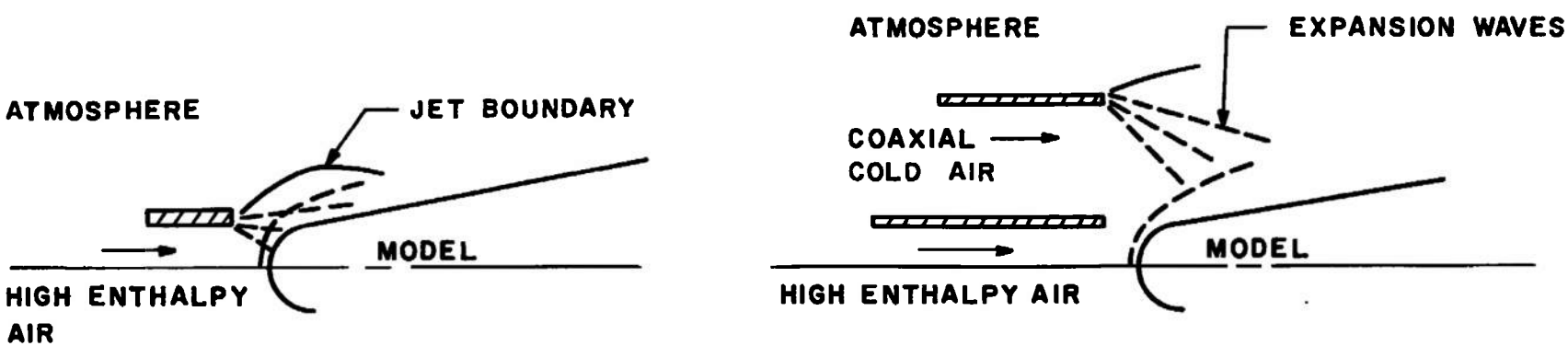

a. Present Testing Technique

b. Coaxial Flow Testing Technique

Fig. 1 Application of the Coaxial Flow Technique to Ablation Testing

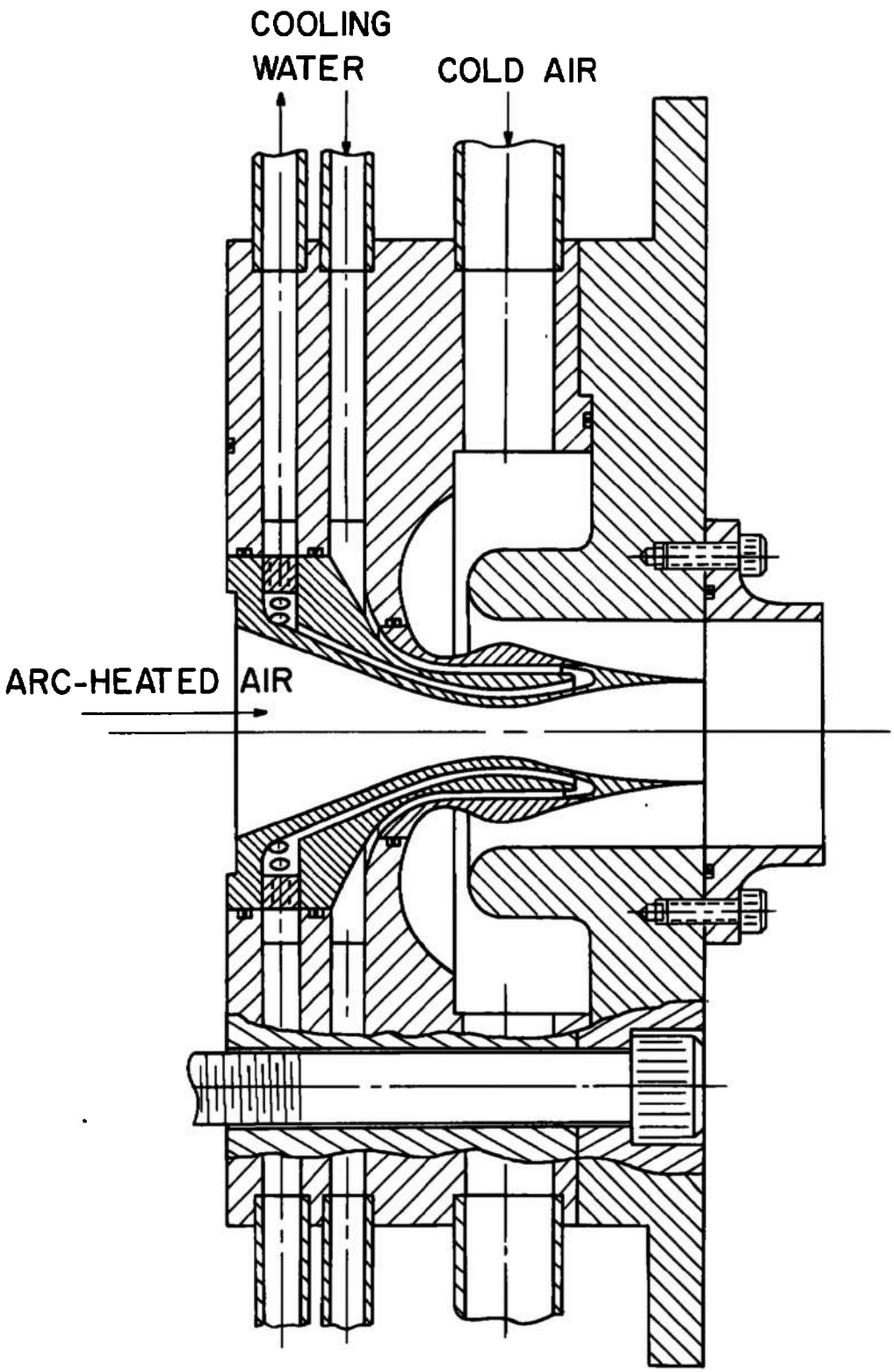

Fig. 2 Coaxial Flow Nozzle Assembly Designed for Arc-Heater Applications

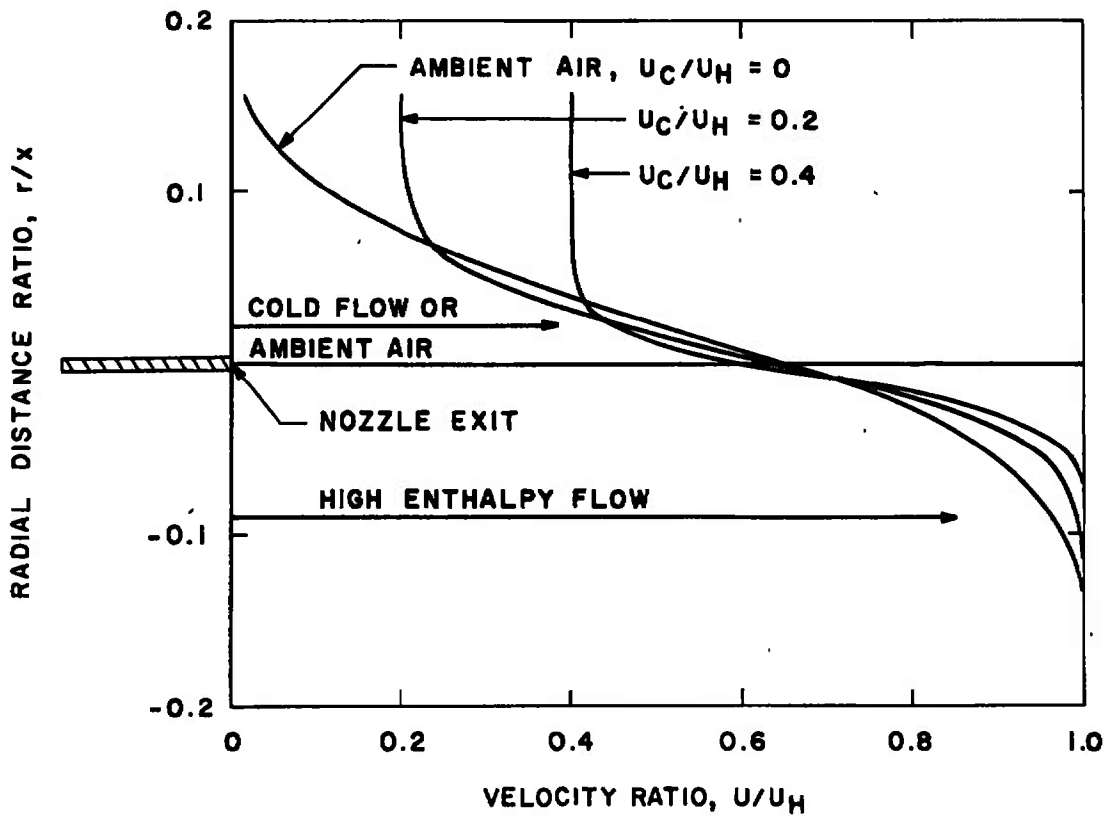

Fig. 3 Effect of Coaxial Flow (Cold Air) on the Spreading of the Velocity Mixing Region for Typical High Enthalpy Applications

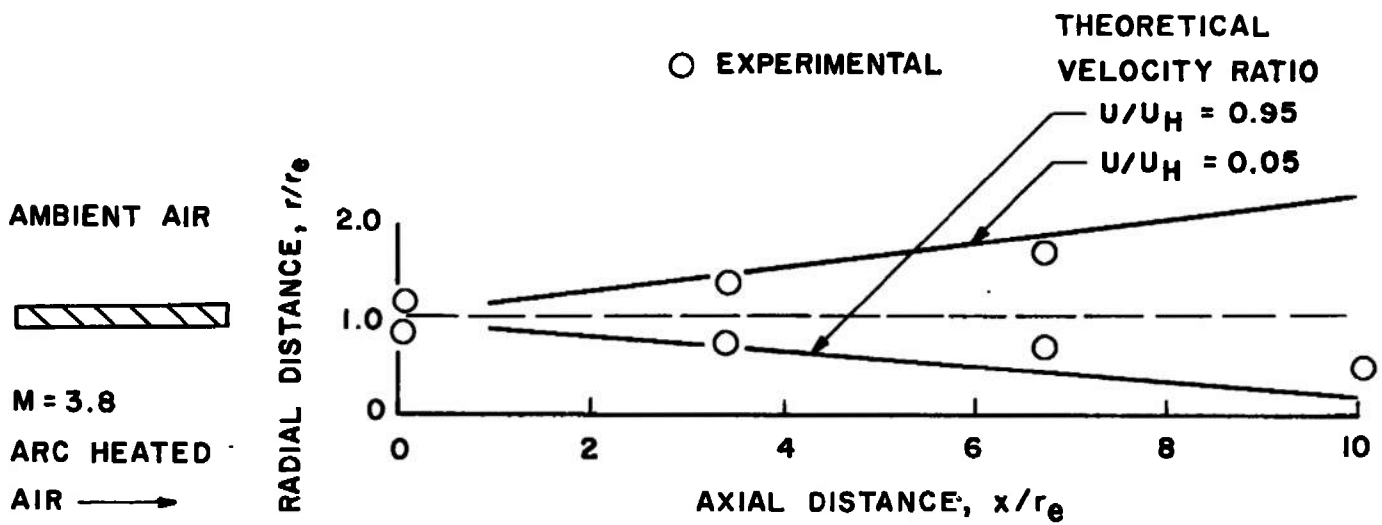

Fig. 4 Comparison of Experimental Data with Theoretical Calculations for the Spread of the Velocity Mixing Region

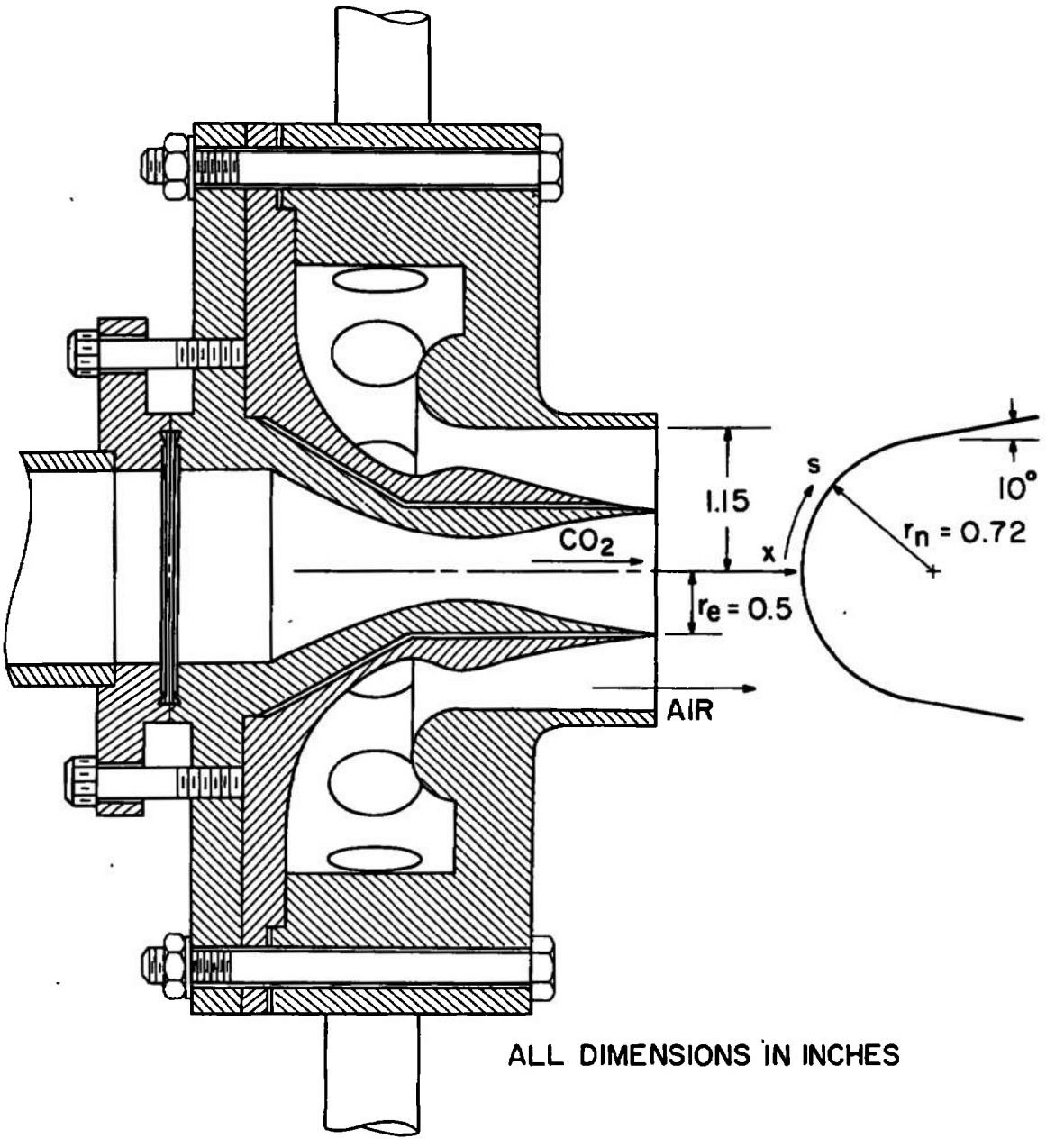

Fig. 5 Coaxial Flow Nozzle Assembly and Reentry Body Model for the Cold Flow Tests

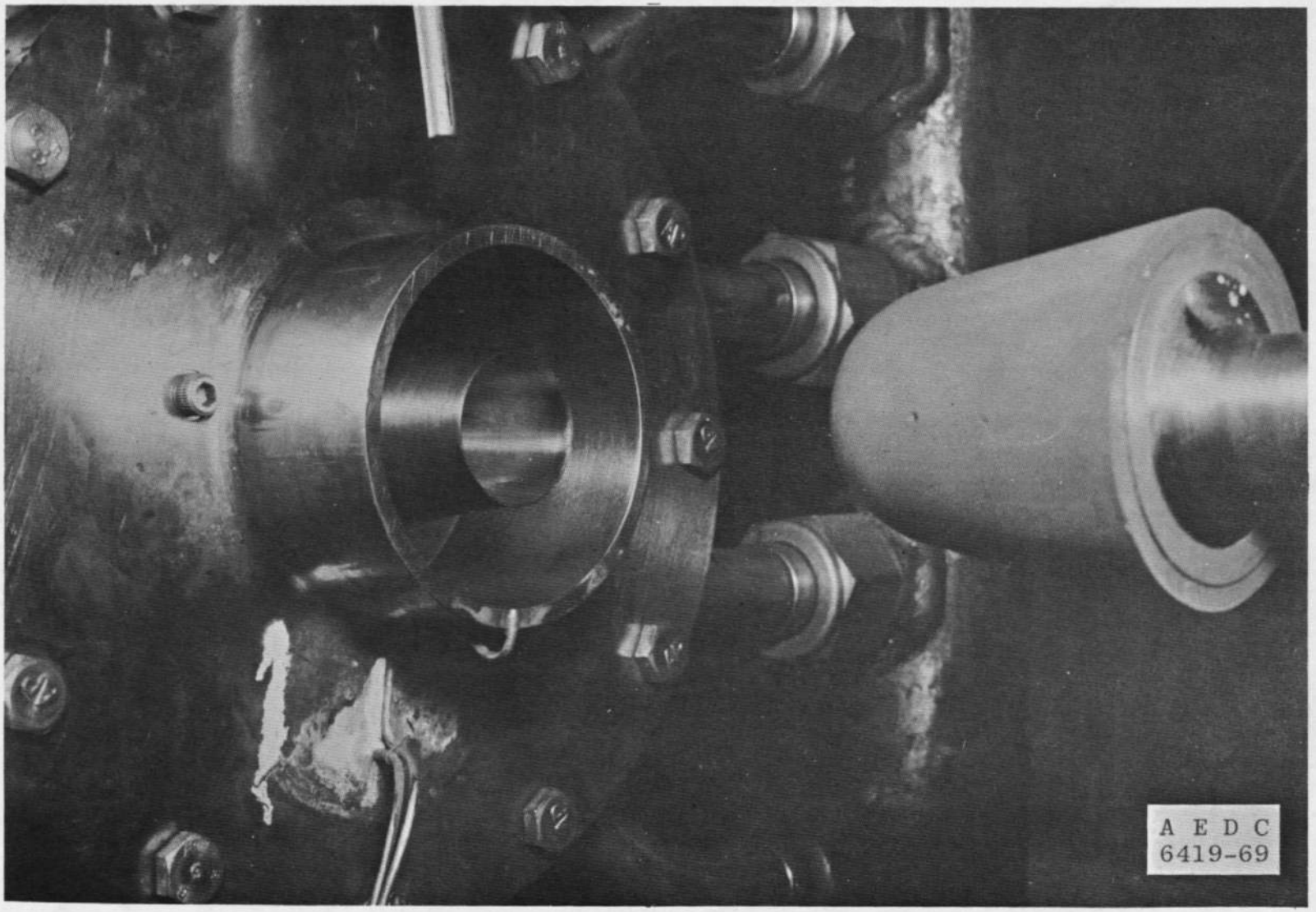

Fig. 6 Coaxial Flow Nozzle and Reentry Body Installation

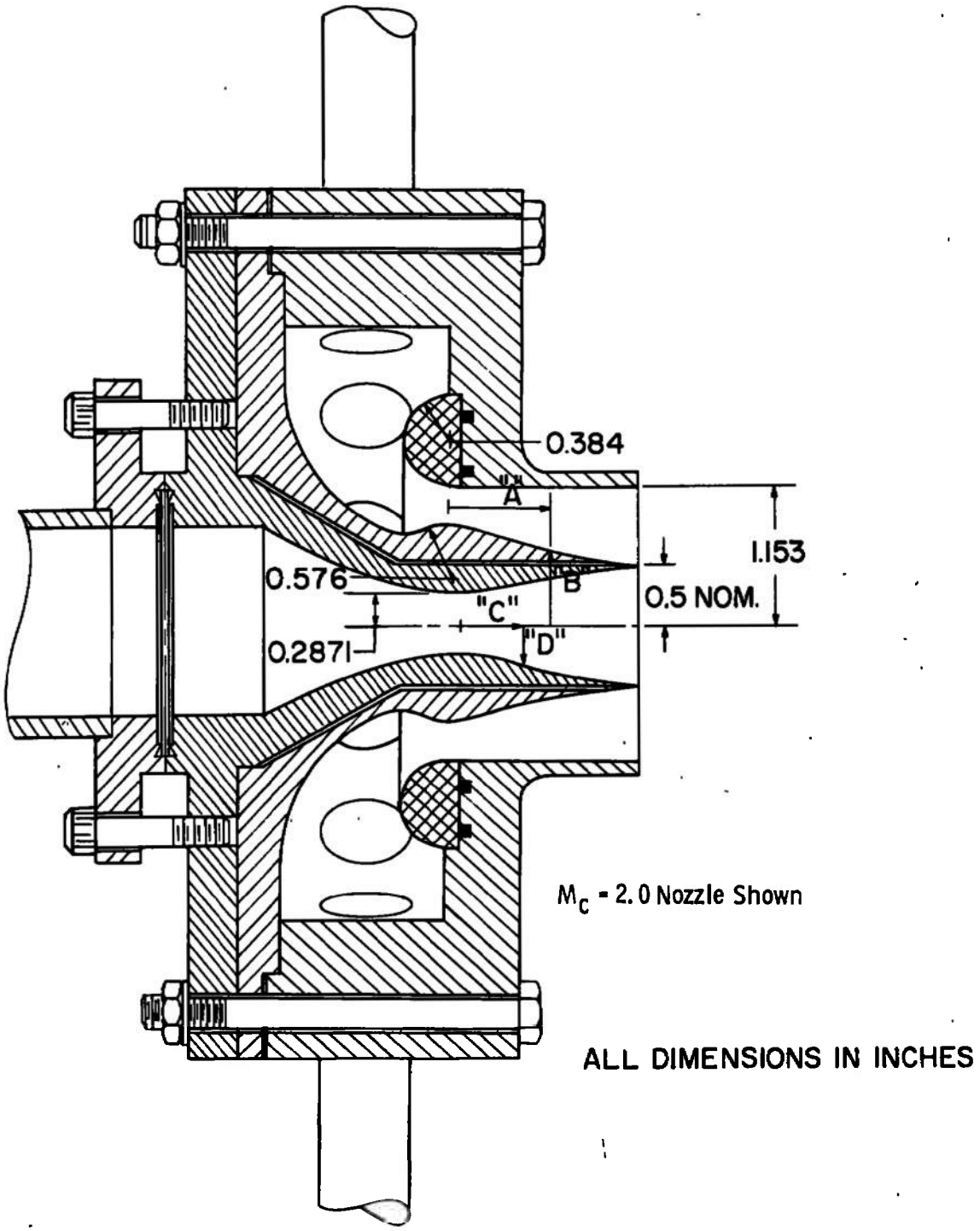

a. Nozzle Assembly

Fig. 7 Coaxial Flow Nozzle Assembly Dimensions and Contours

Air Nozzle Design M_C = 2.0		Air Nozzle Design M_C = 2.5		CO_2 Nozzle Design		CO_2 Nozzle "As Built"	
"A"	"B"	"A"	"B"	"C"	"D"	"C"	"D"
0	0.8433	0	0.9573	0	0.2871	0	0.2865
0.0506	0.8411	0.0605	0.9555	0.0904	0.2905	0.1	0.2887
0.1009	0.8340	0.1095	0.9513	0.1928	0.3081	0.2	0.2958
0.1528	0.8211	0.1582	0.9451	0.2828	0.3284	0.3	0.3086
0.1990	0.8077	0.2059	0.9372	0.3770	0.3499	0.4	0.3266
0.2452	0.7938	0.2612	0.9248	0.4276	0.3611	0.5	0.3469
0.3336	0.7669	0.3090	0.9097	0.4810	0.3726	0.6	0.3678
0.4455	0.7333	0.3614	0.8903	0.5373	0.3842	0.7	0.3877
0.5861	0.6925	0.3995	0.8764	0.5966	0.3959	0.8	0.4053
0.7225	0.6566	0.4642	0.8533	0.6589	0.4074	0.9	0.4198
0.8691	0.6216	0.5049	0.8391	0.7242	0.4187	1.0	0.4321
0.9144	0.6117	0.5466	0.8248	0.7924	0.4295	1.1	0.4426
0.9692	0.6002	0.6308	0.7969	0.8633	0.4398	1.2	0.4526
1.0437	0.5859	0.7115	0.7715	0.9366	0.4494	1.3	0.4627
1.1372	0.5694	0.8446	0.7319	1.0121	0.4583	1.4	0.4731
1.2330	0.5546	0.9567	0.7012	1.0892	0.4662	1.5	0.4831
1.3279	0.5416	1.0948	0.6664	1.1676	0.4733		
1.4208	0.5309	1.1768	0.6475	1.2469	0.4795		
1.5101	0.5224	1.2697	0.6276	1.3264	0.4847		
1.5944	0.5157	1.3802	0.6057	1.4058	0.4890		
1.6726	0.5110	1.5181	0.5815				
		1.6912	0.5562				
		1.9098	0.5312				
		2.1573	0.5123				
		2.2607	0.5072				

All dimensions in inches.

b. Nozzle Coordinates

Fig. 7 Concluded

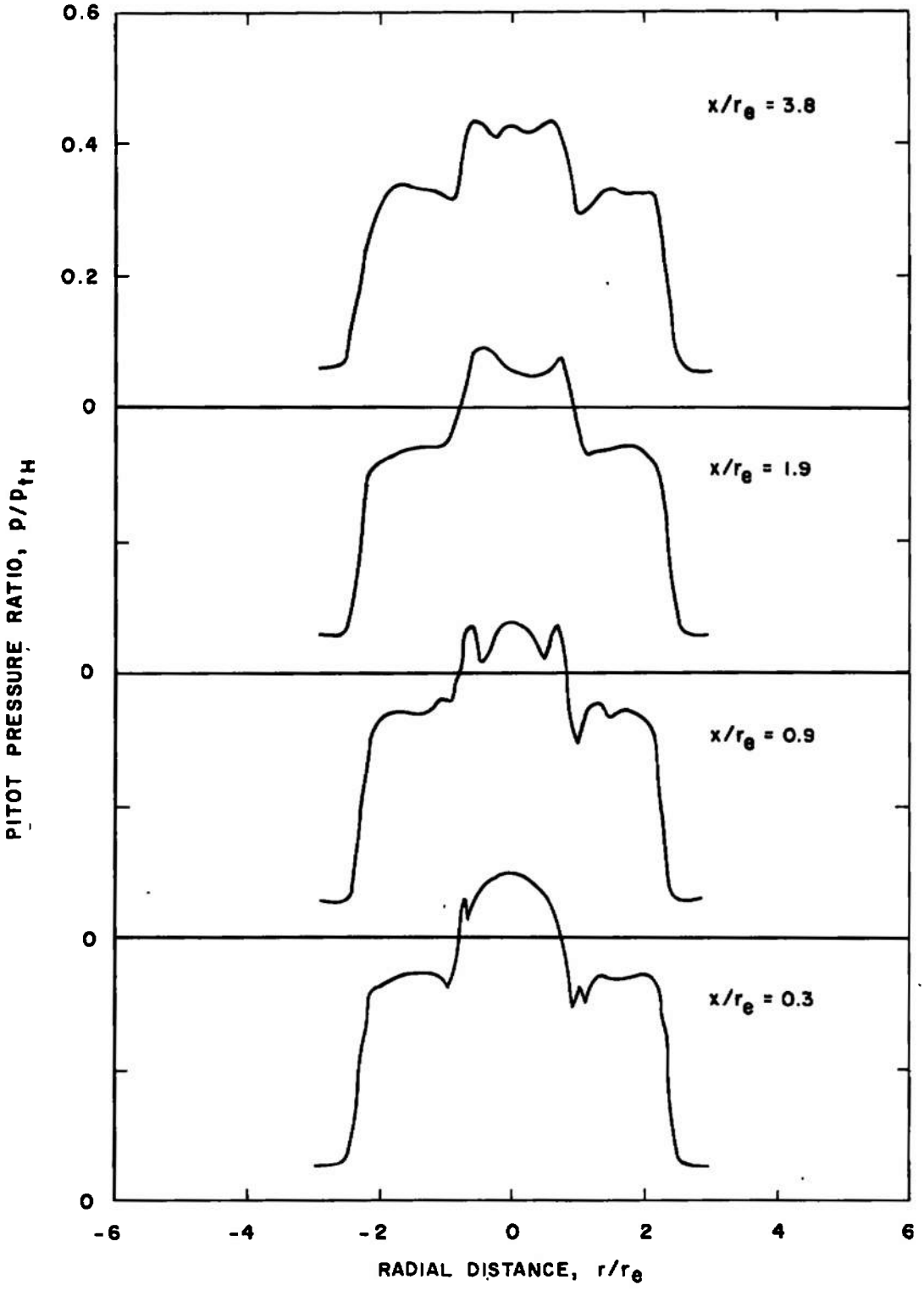

a. $M_c = 2.0$

Fig. 8 Pitot Pressure Distribution of the Coaxial Flow Fields, $p_H/p_\infty = 1$

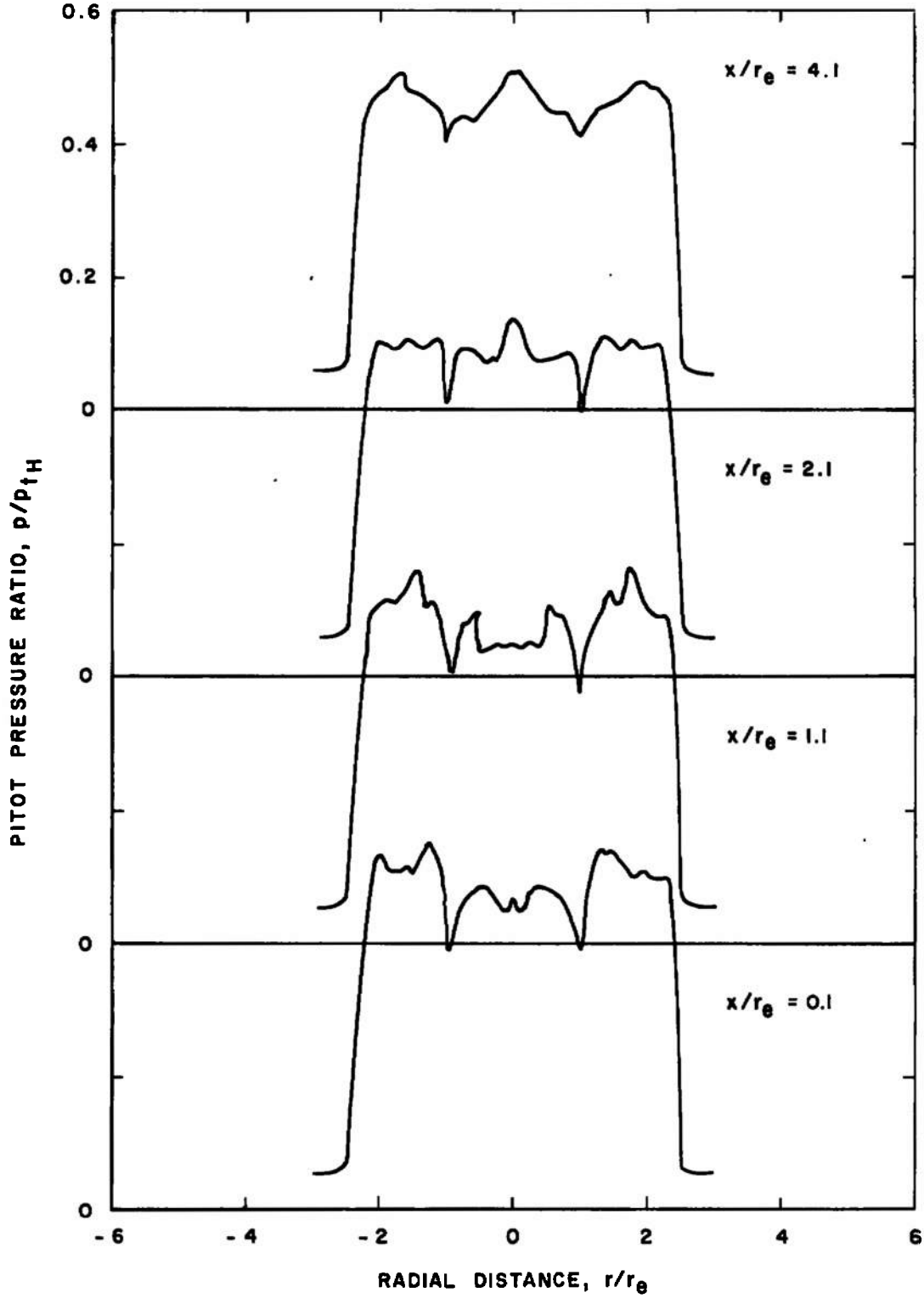

b. $M_c = 2.5$

Fig. 8 Concluded

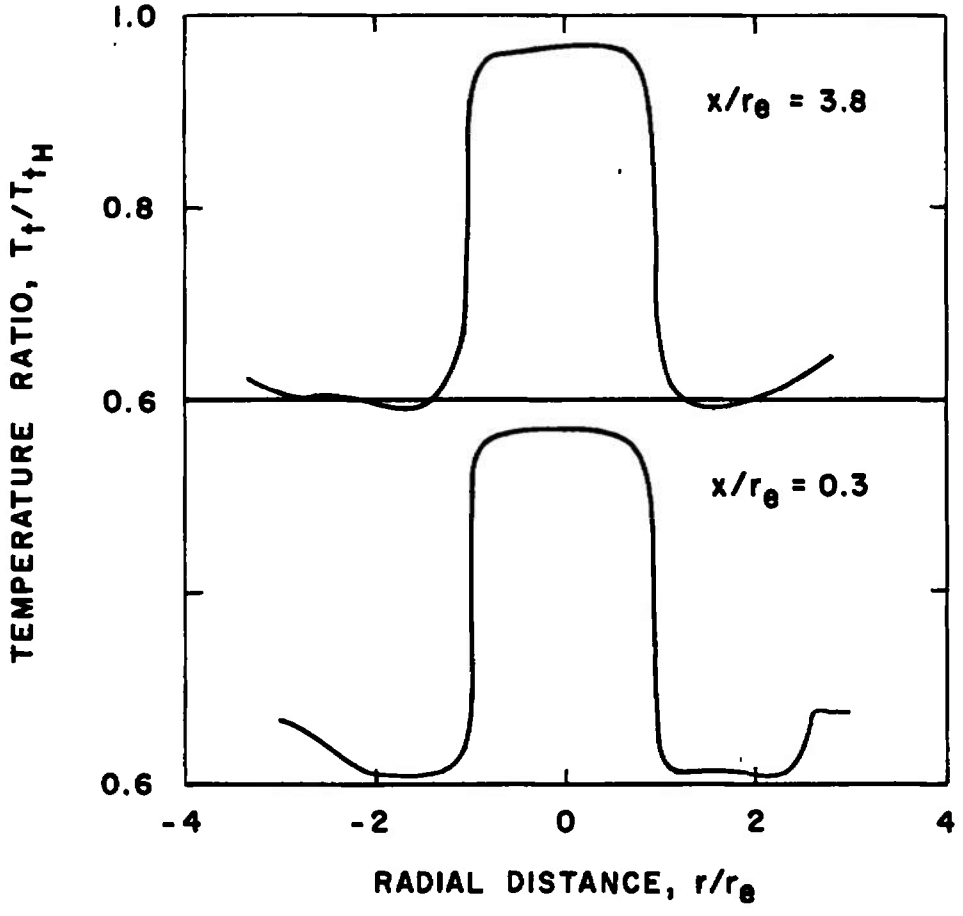

Fig. 9 Stagnation Temperature Distribution of the Coaxial Flow Field, $M_c = 2.0$ and $p_H/p_\infty = 1$

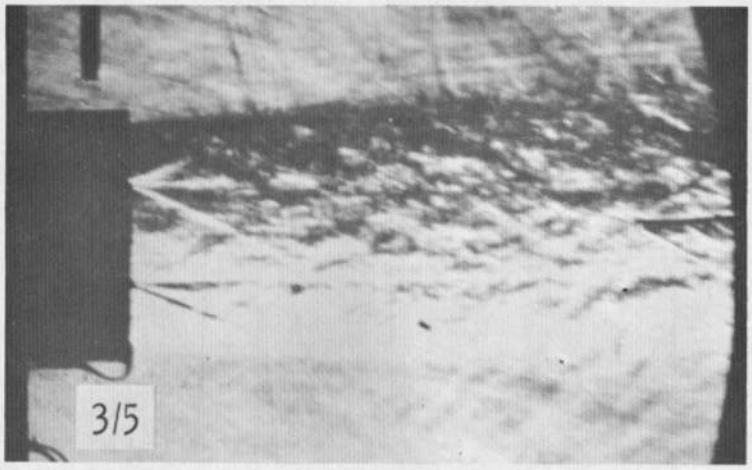

a. $M_c = 2.5$

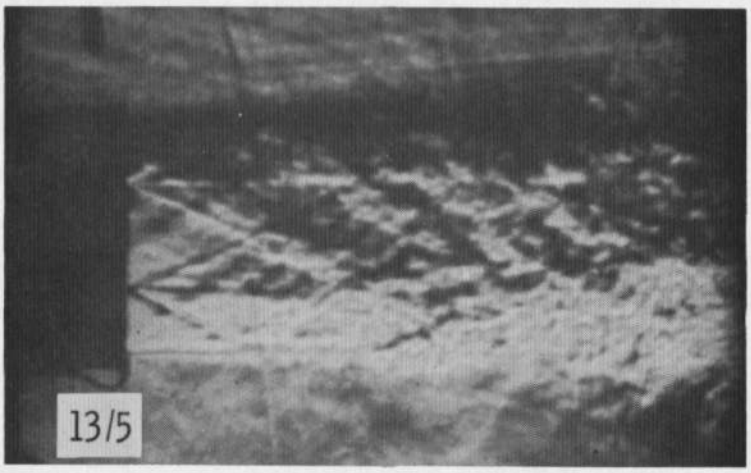

b. $M_c = 2.0$

Fig. 10 Schlieren Photographs of the Coaxial Flow Fields, $p_H/p_\infty = 1$

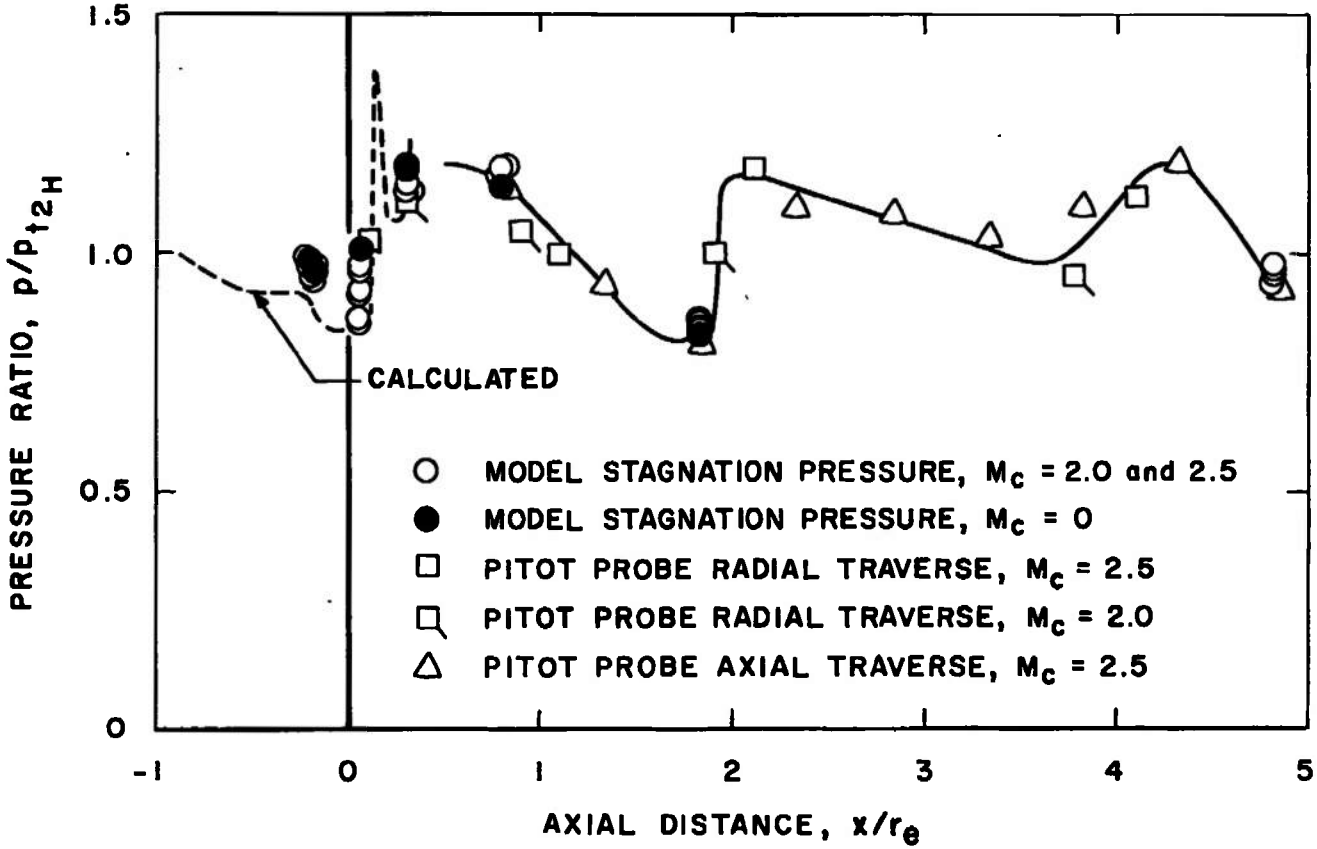

Fig. 11 Compilation of Model and Pitot Probe Data on the Nozzle Centerline

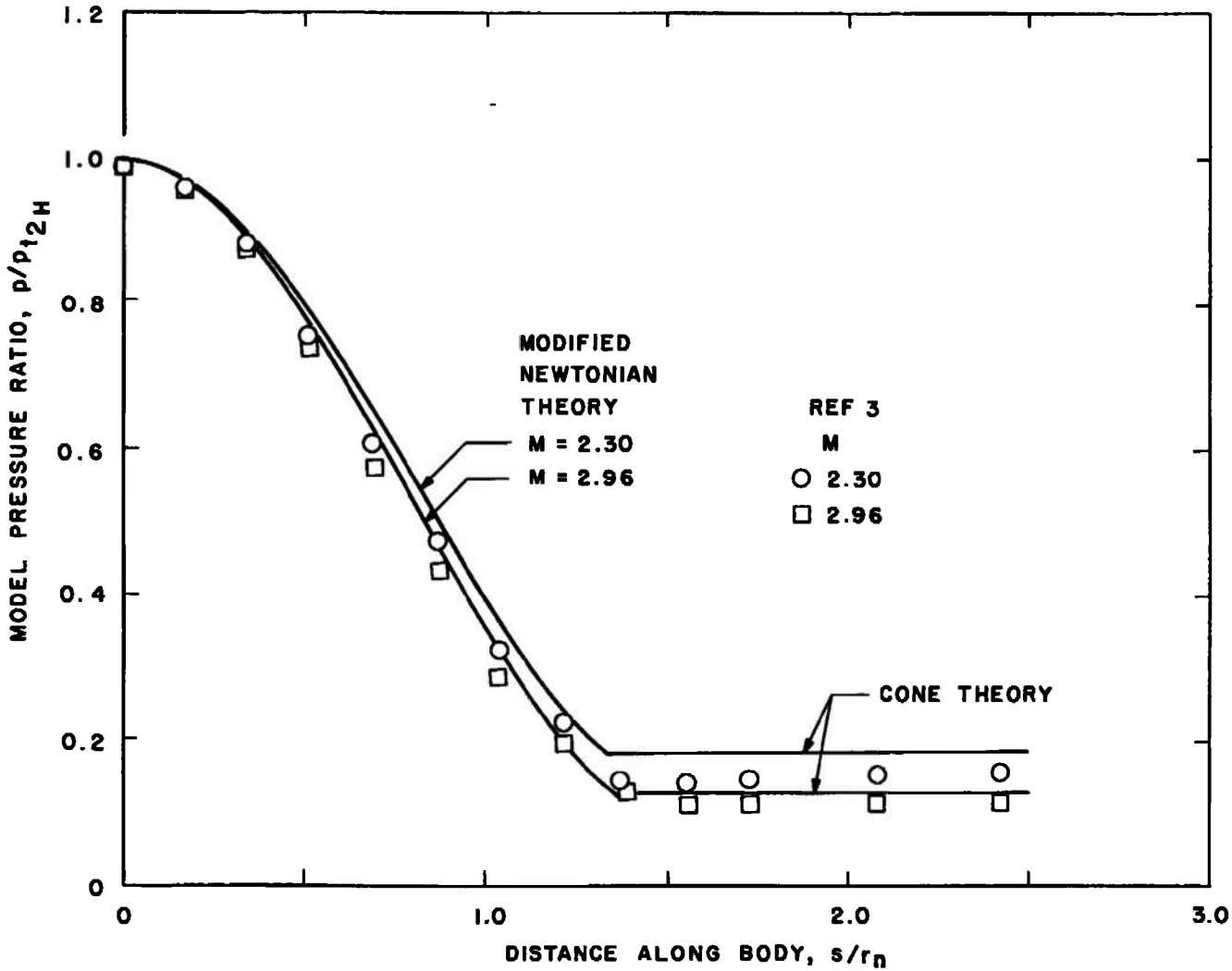

Fig. 12 Comparison of Theory and Wind-Tunnel Data for a Sphere-9-deg Cone Body

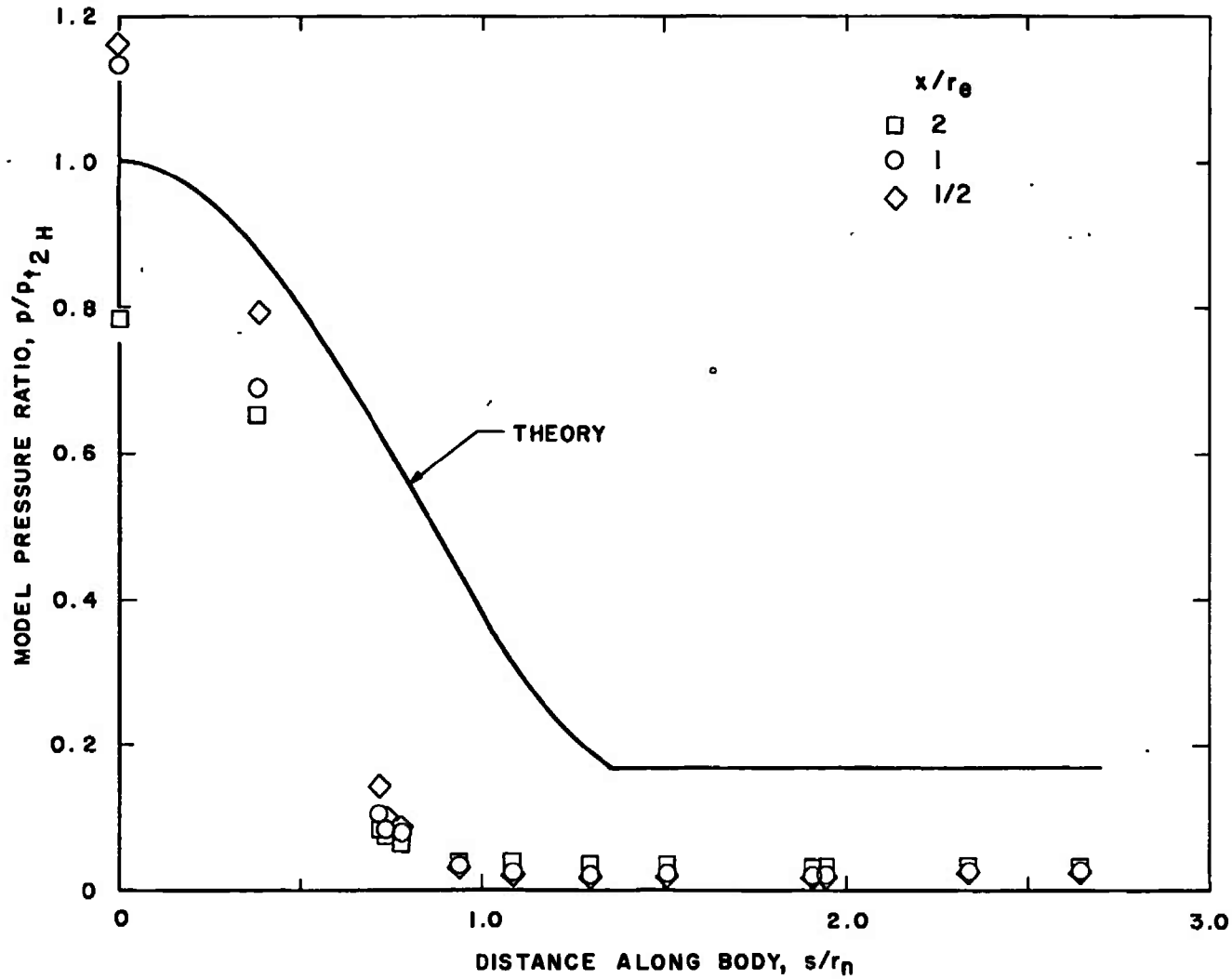

Fig. 13 Model Pressure Distribution without the Coaxial Air Jet, $p_H/p_\infty = 6$

$x/r_e = 2$ $x/r_e = 1$ $x/r_e = 1/2$

Fig. 14 Schlieren Photographs of the Flow Fields Corresponding to Fig. 13

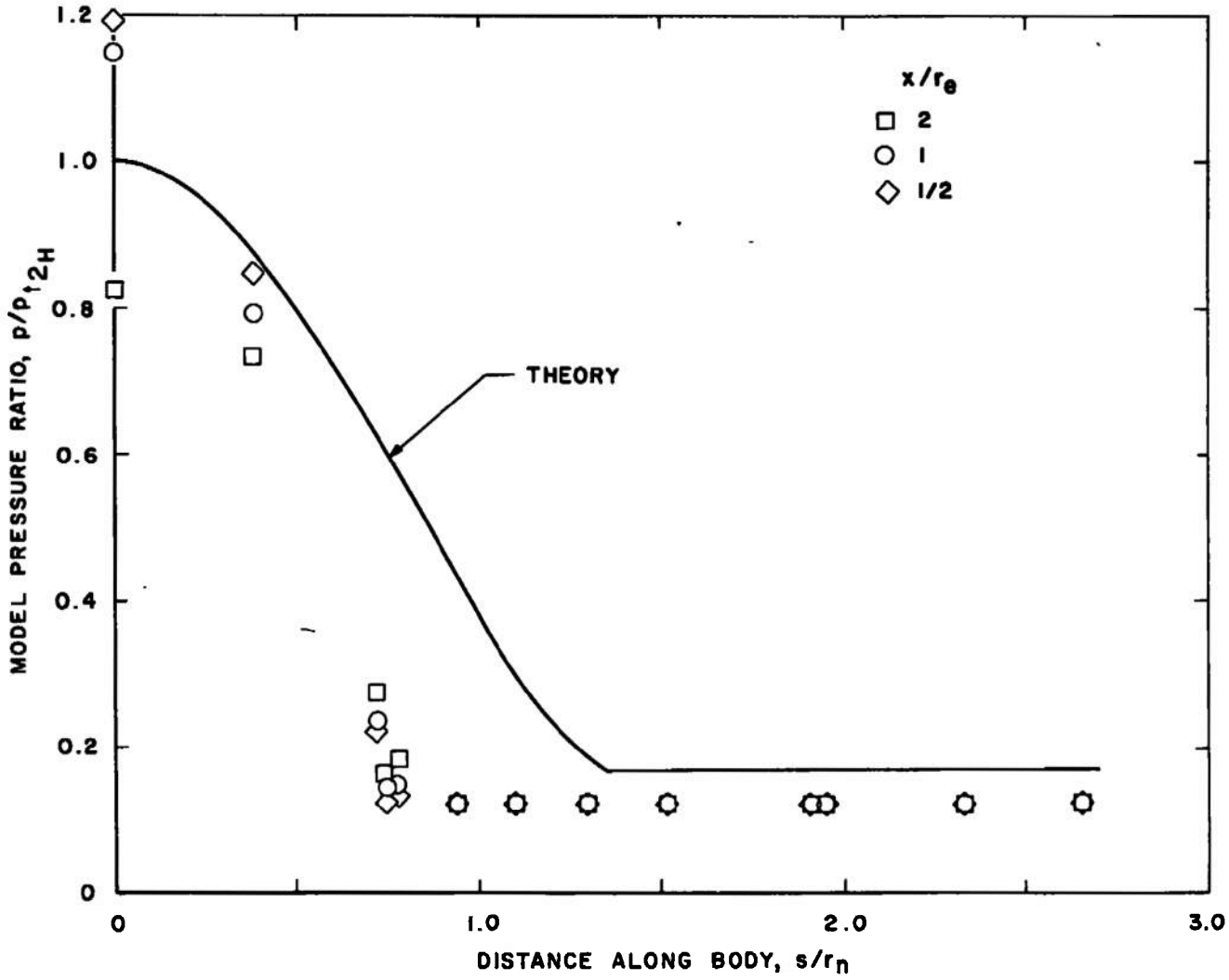

Fig. 15 Model Pressure Distributions without the Coaxial Air Jet, $p_H/p_\infty = 1$

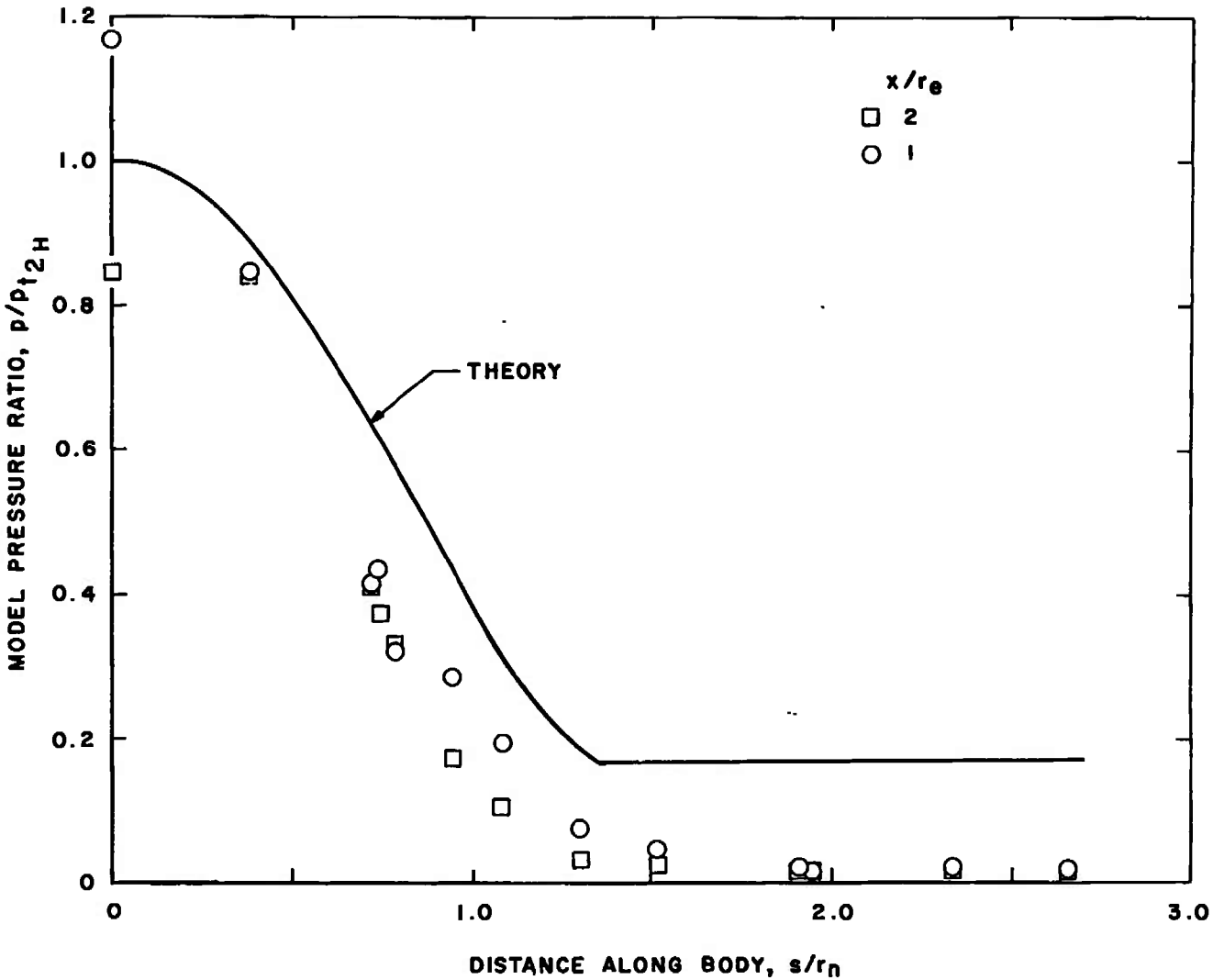

Fig. 16 Model Pressure Distributions with the Coaxial Air Jet, M_c = 2.0 and p_H/p_∞ = 6

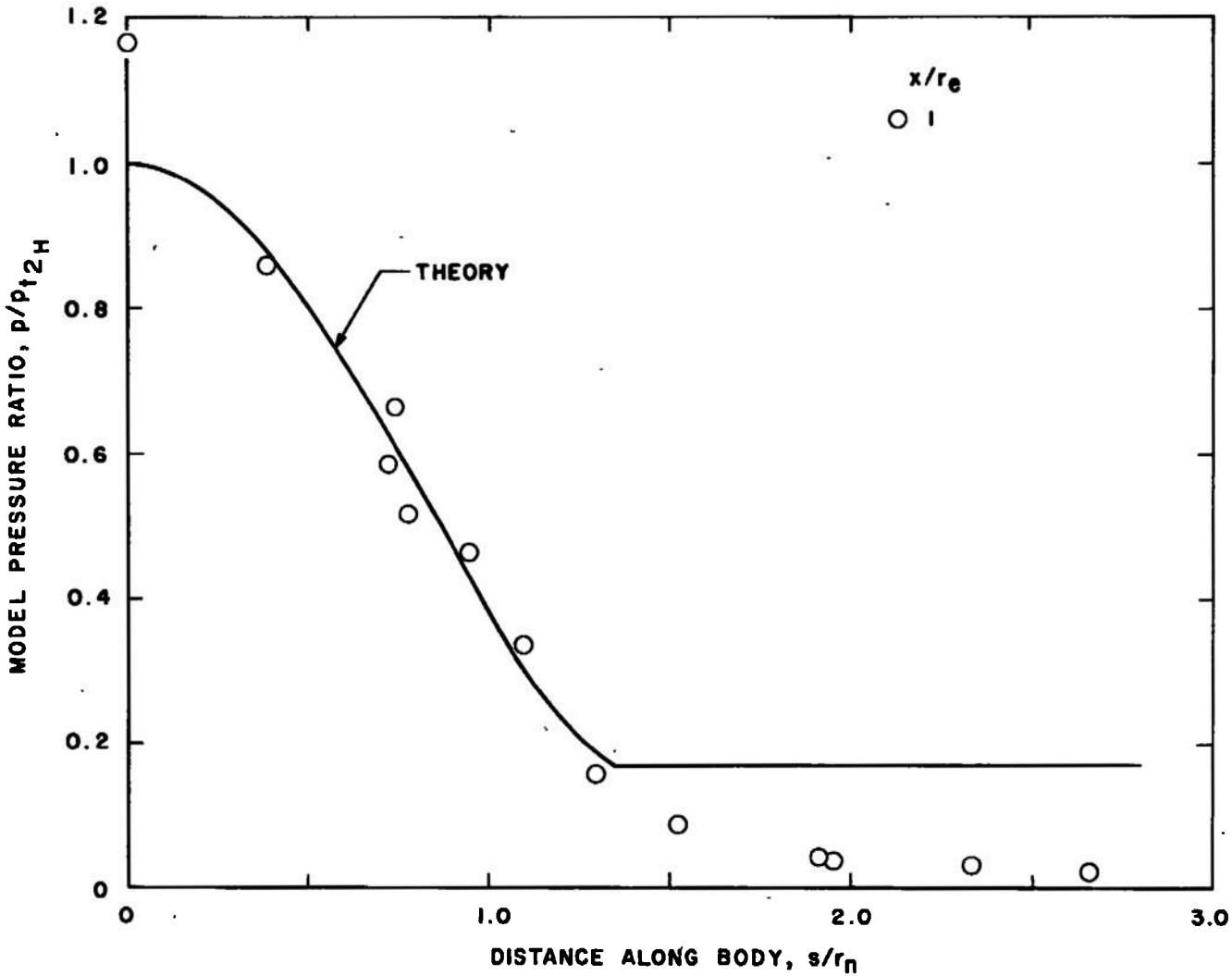

Fig. 17 Model Pressure Distribution with the Coaxial Air Jet, $M_c = 2.5$, $p_H/p_\infty = 6$

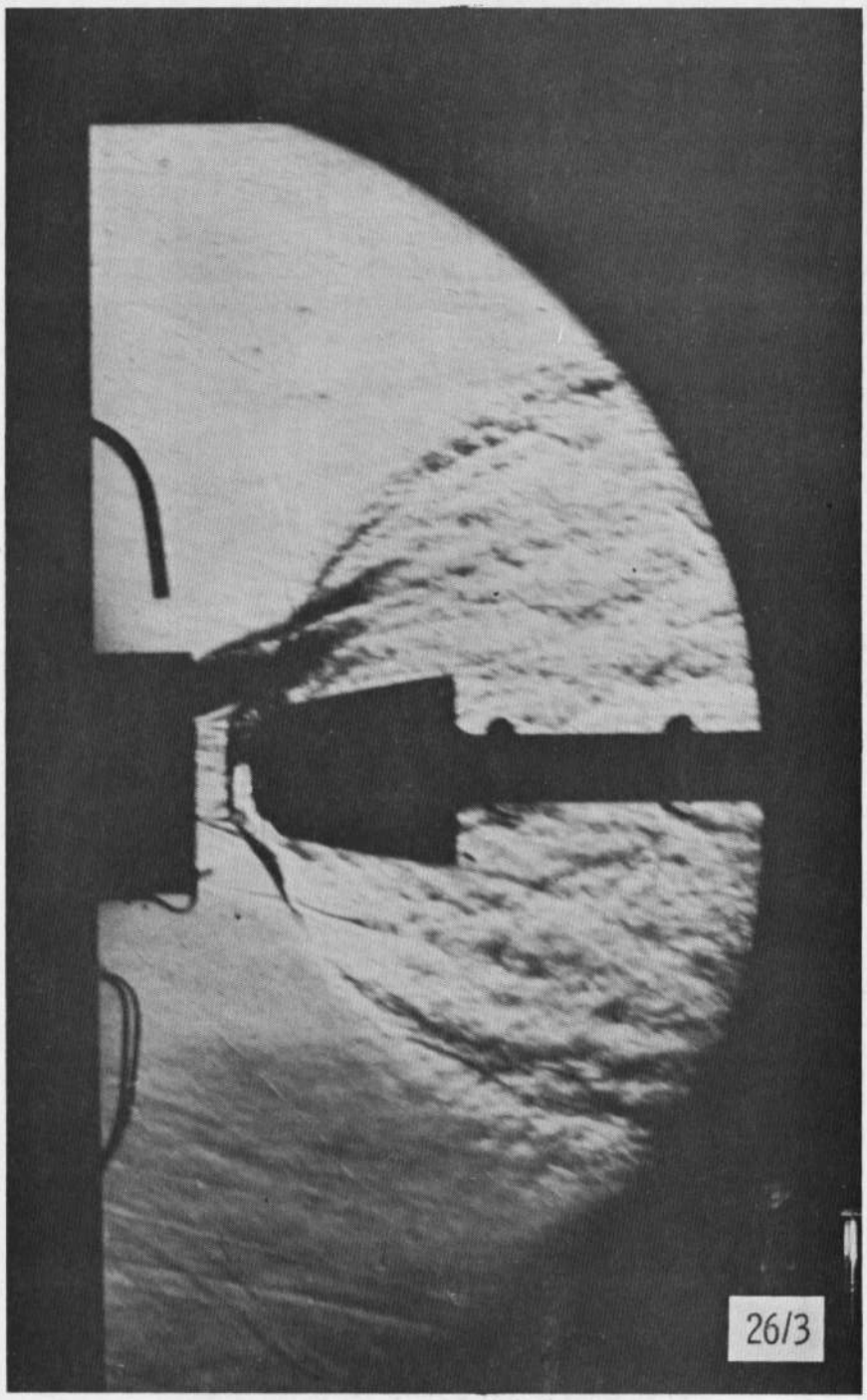

Fig. 18 Schlieren Photograph of the Flow Field Corresponding to Fig. 17, $M_c = 2.5$, $p_H/p_\infty = 6$

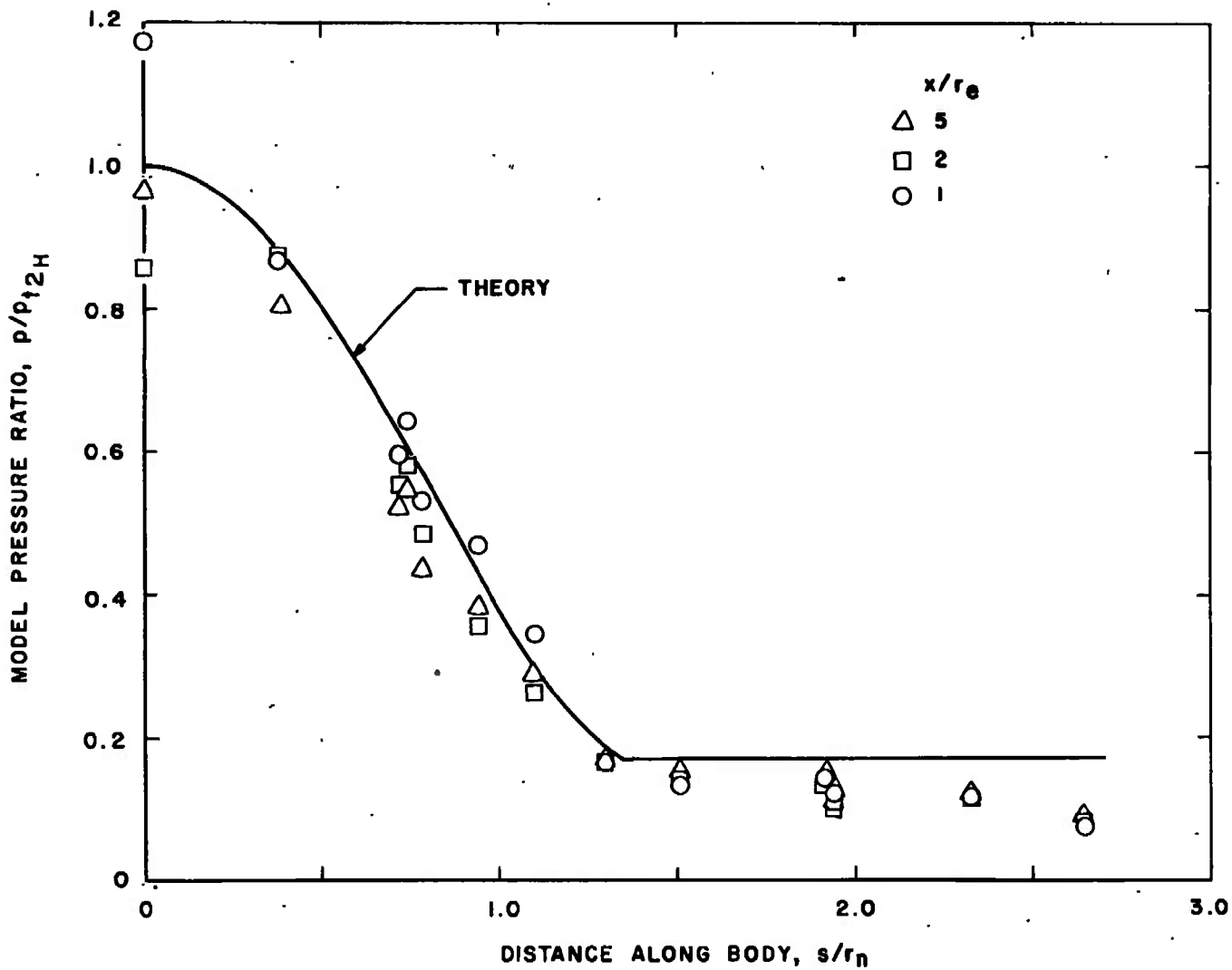

Fig. 19 Model Pressure Distributions with the Coaxial Air Jet Simulating Tests in a Pressurized Tank, $M_c = 2.5$, $p_H/p_\infty = 1$

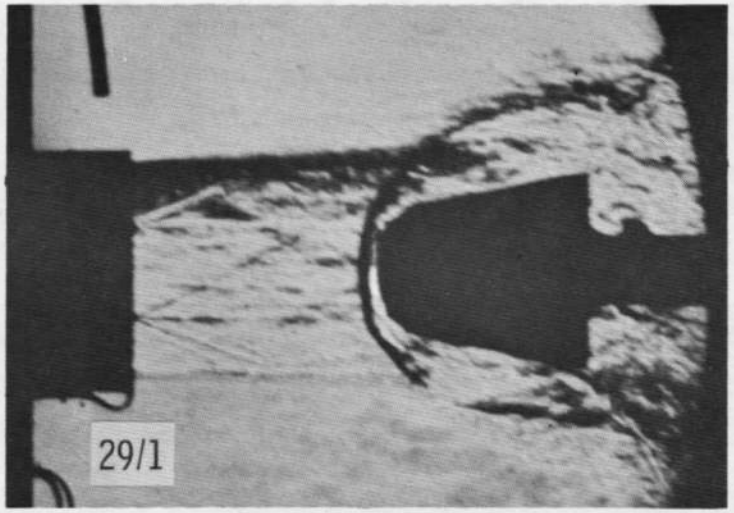

$x/r_e = 5$

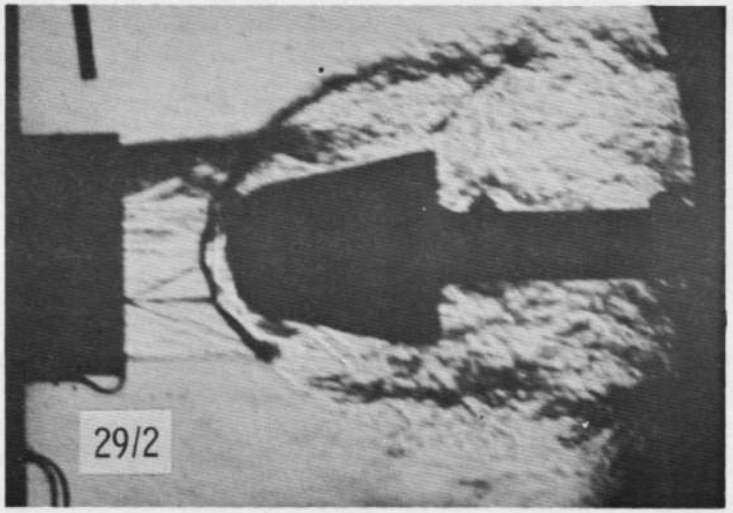

$x/r_e = 2$

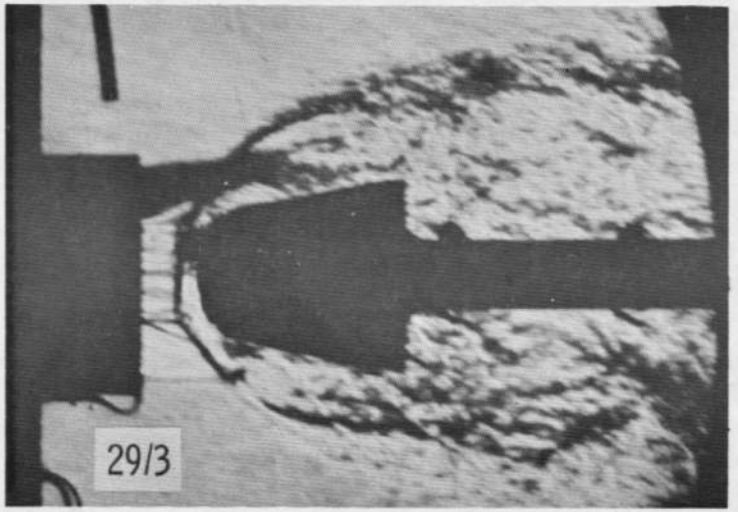

$x/r_e = 1$

Fig. 20 Schlieren Photographs of the Flow Fields Corresponding to Fig. 19, $M_c = 2.5$, $p_H/p_\infty = 1$

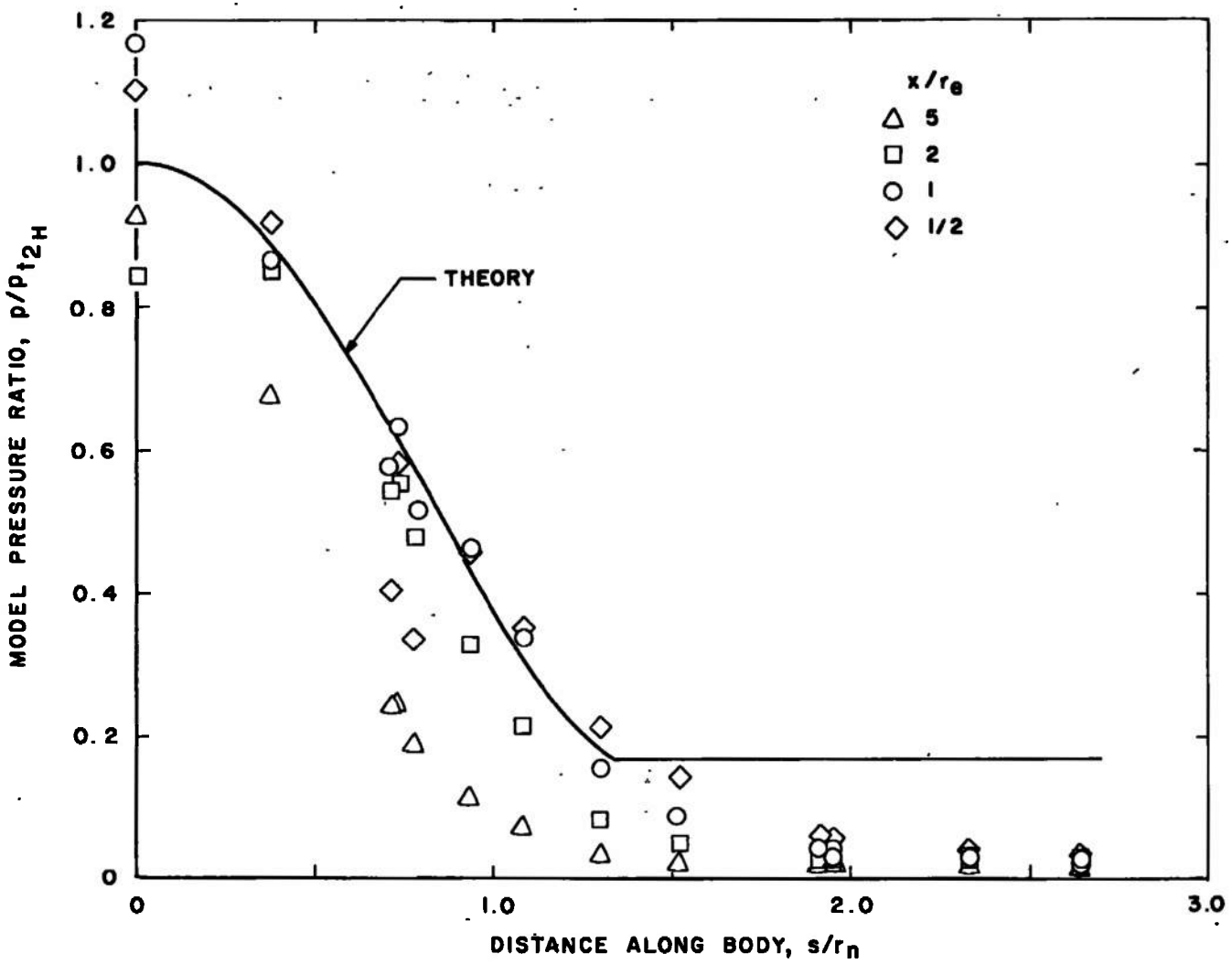

Fig. 21 Effect of Axial Location on the Model Pressure Distribution with the Coaxial Air Jet, $M_c = 2.5$ and $p_H/p_\infty = 6$

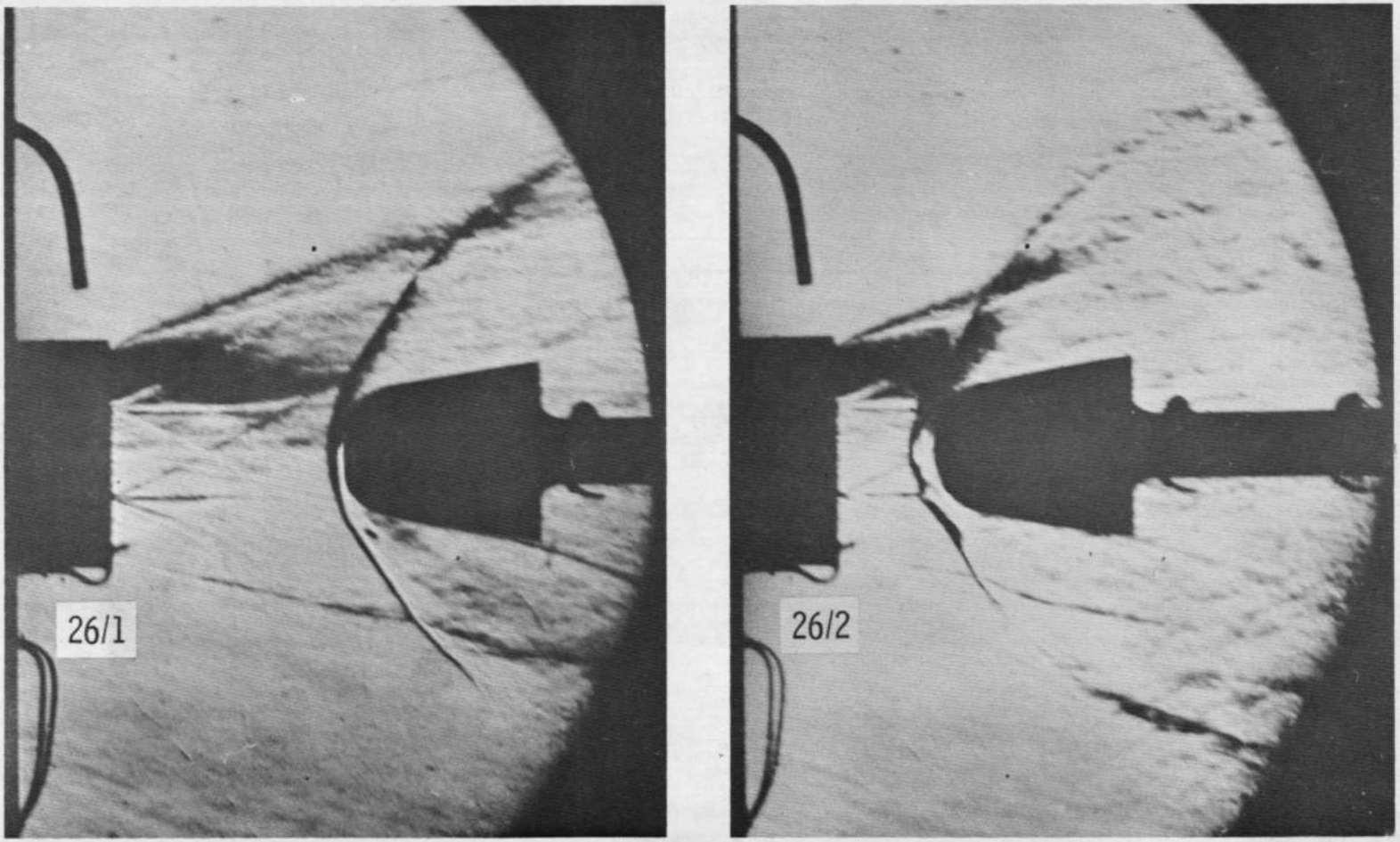

$x/r_e = 5$ $x/r_e = 2$

Fig. 22 Schlieren Photographs of the Flow Fields Corresponding to Fig. 21, $M_c = 2.5$, $p_H/p_\infty = 6$

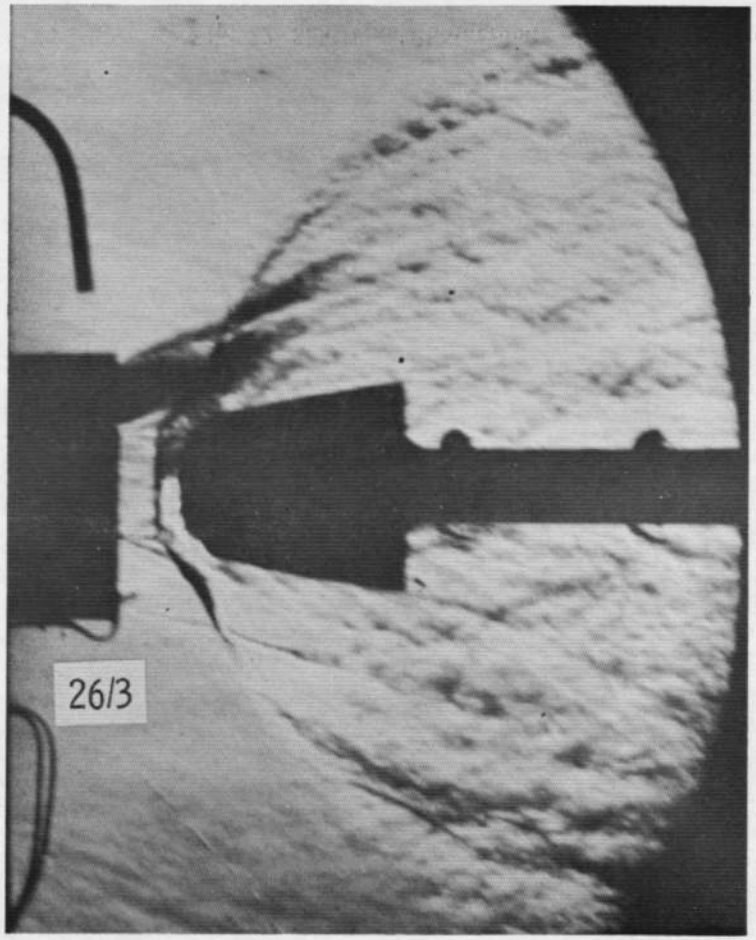

$x/r_e = 1$

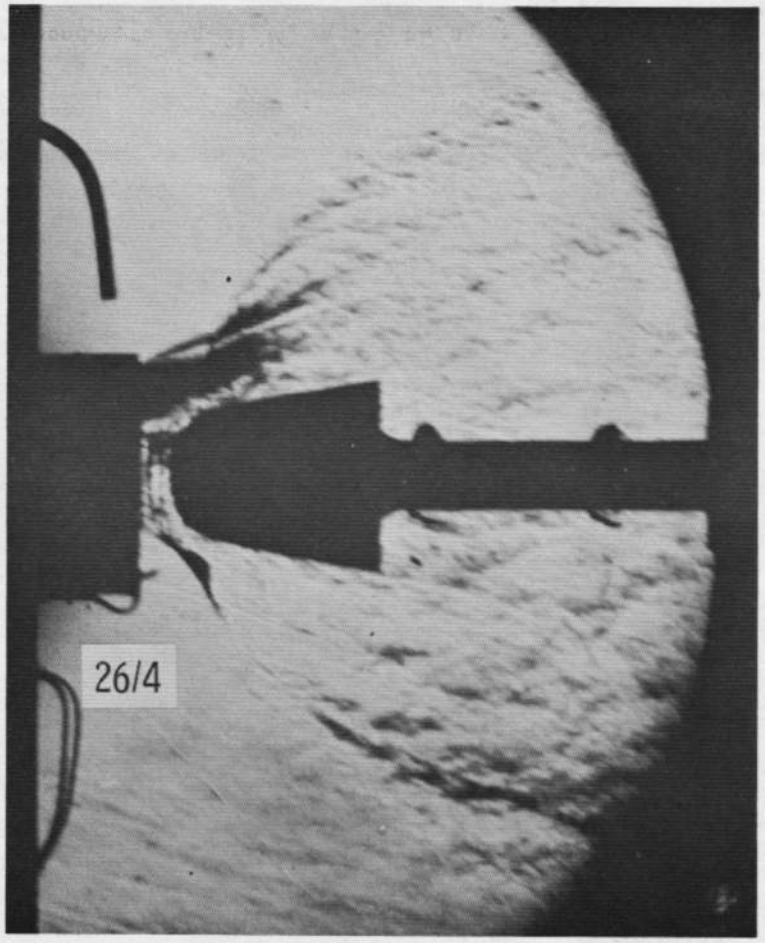

$x/r_e = 1/2$

Fig. 22 Concluded

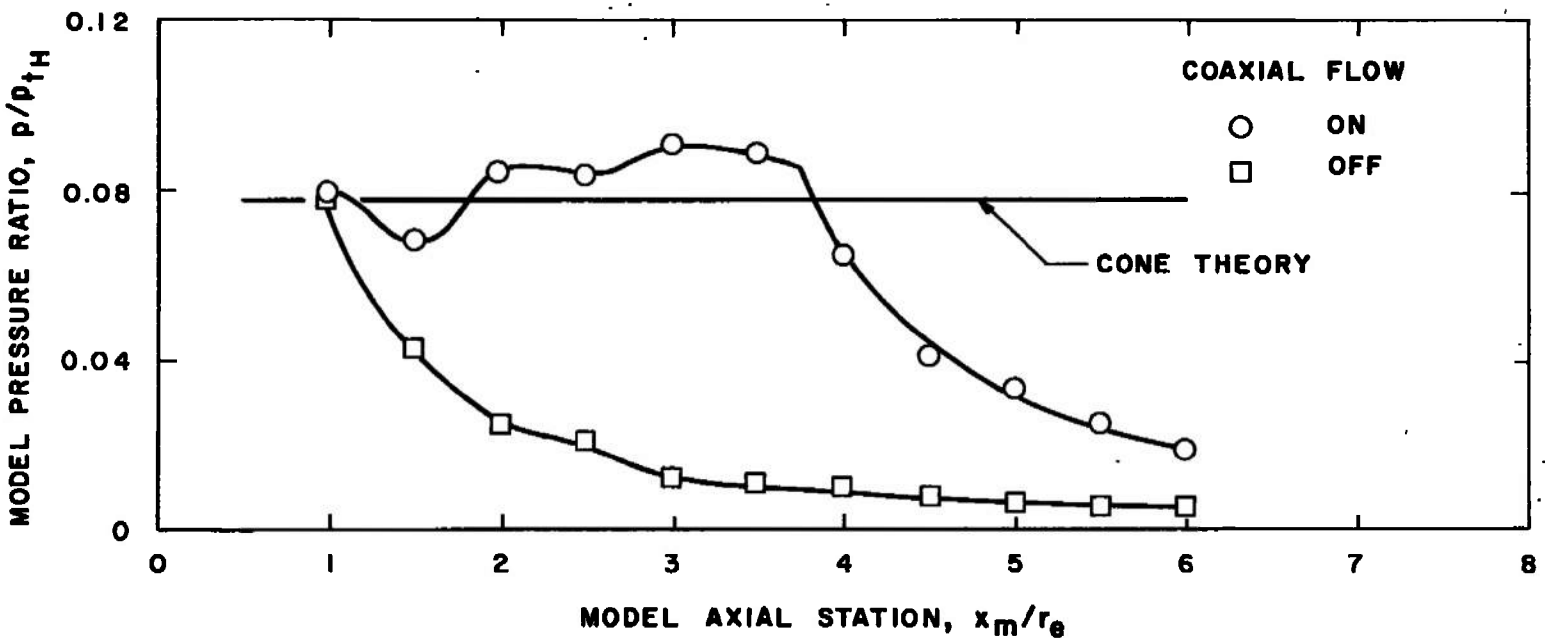

a. $M_c \sim 2.5$

Fig. 23 Effect of the Coaxial Air Jet on the Pressure Distributions on a Sharp 10-deg Cone, $p_H/p_\infty = 6$ and $x/r_e = 0$

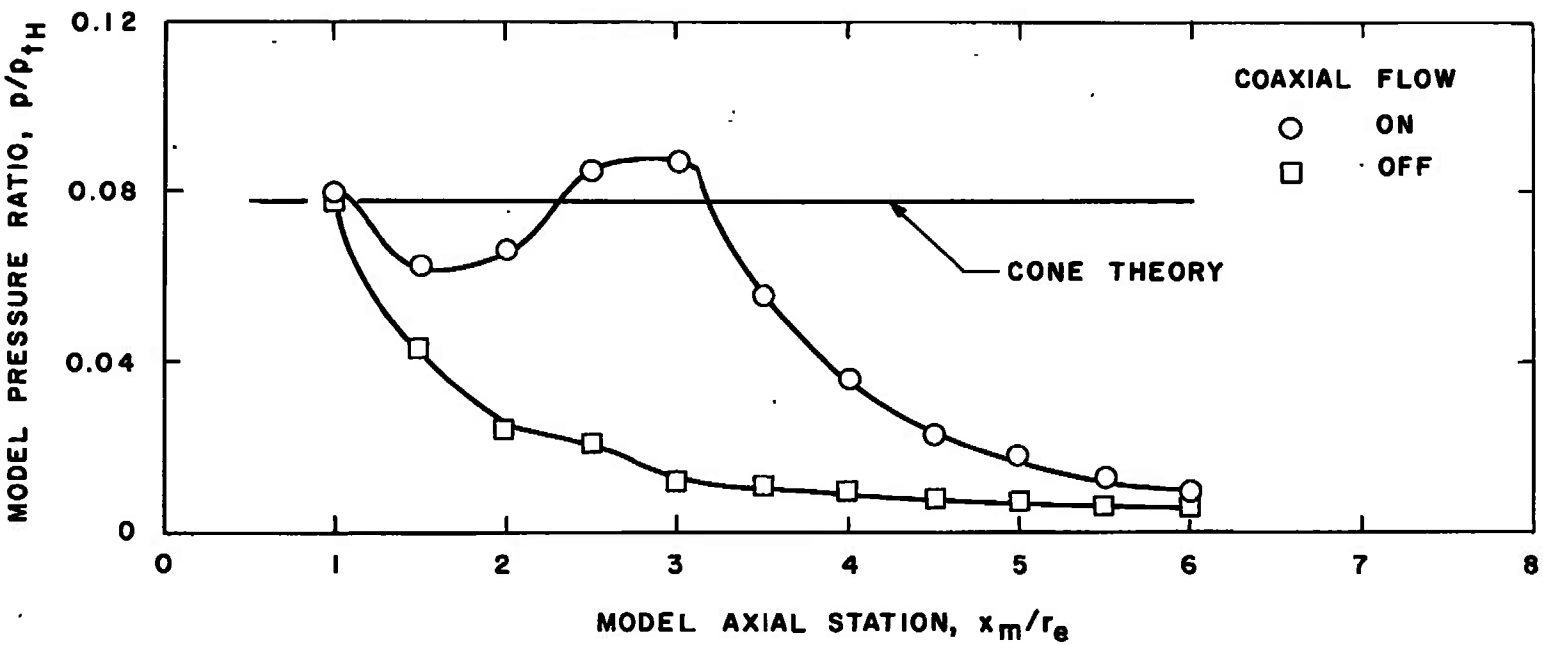

b. $M_c = 2.0$

Fig. 23 Concluded

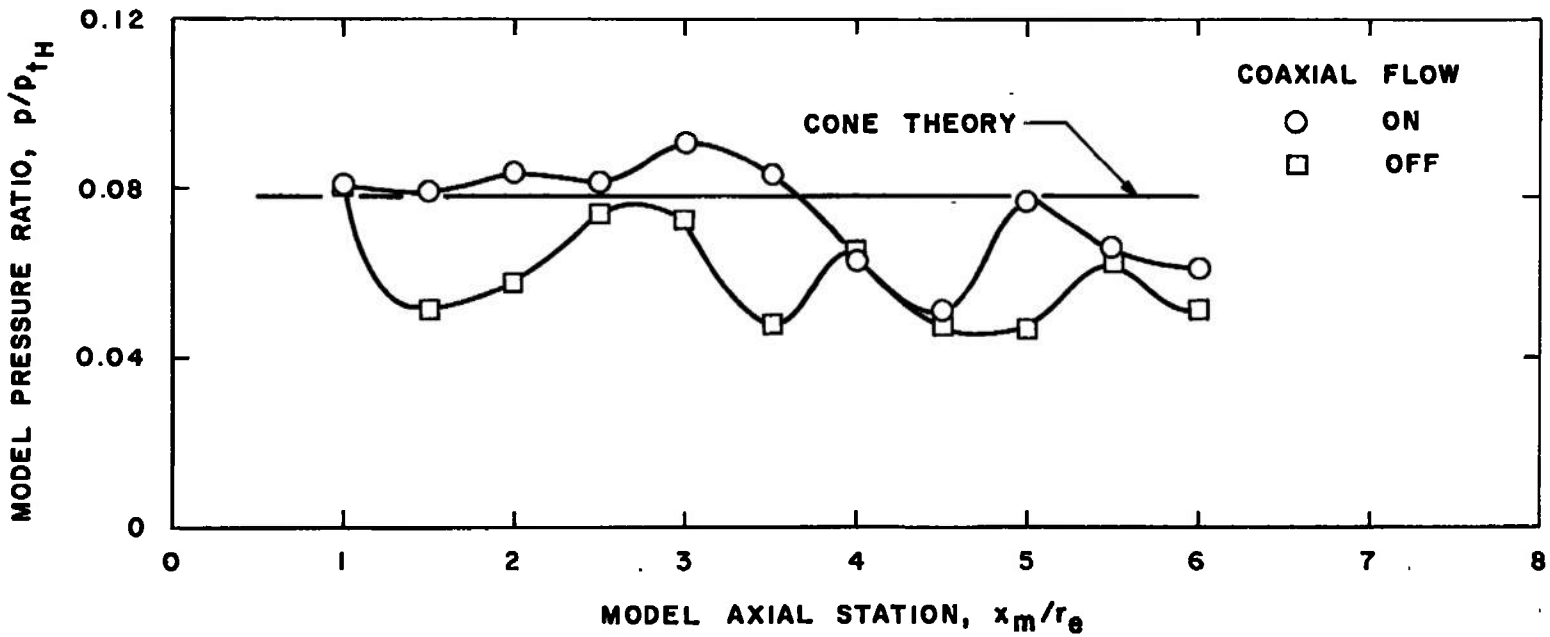

Fig. 24 Effect of the Coaxial Air Jet on the Pressure Distributions on a Sharp 10-deg Cone, $p_H/p_\infty = 1$, $x/r_e = 0$, and $M_c = 2.5$

UNCLASSIFIED

Security Classification

DOCUMENT CONTROL DATA - R & D

(Security classification of title, body of abstract and indexing annotation must be entered when the overall report is classified)

1. ORIGINATING ACTIVITY *(Corporate author)*
Arnold Engineering Development Center
ARO, Inc., Operating Contractor
Arnold Air Force Station, Tennessee 37389

2a. REPORT SECURITY CLASSIFICATION
UNCLASSIFIED

2b. GROUP
N/A

3. REPORT TITLE
ABLATION TESTING IN HOT AND COLD COAXIAL JETS - PHASE I, COLD FLOW FEASIBILITY TESTS

4. DESCRIPTIVE NOTES *(Type of report and inclusive dates)*
Final Report July 1968 to November 1969

5. AUTHOR(S) *(First name, middle initial, last name)*
R. D. Herron, ARO, Inc.

6. REPORT DATE	7a. TOTAL NO. OF PAGES	7b. NO. OF REFS
April 1970	50	5

8a. CONTRACT OR GRANT NO.	9a. ORIGINATOR'S REPORT NUMBER(S)
AF40600-69-C-0001	AEDC-TR-70-64
b. PROJECT NO. 8950	
c. Task 12	9b. OTHER REPORT NO(S) *(Any other numbers that may be assigned this report)*
d. Program Element 62201F	N/A

10. DISTRIBUTION STATEMENT
This document has been approved for public release and sale; its distribution is unlimited.

11. SUPPLEMENTARY NOTES	12. SPONSORING MILITARY ACTIVITY
Available in DDC.	Arnold Engineering Development Center, Air Force Systems Command, Arnold AF Station, Tenn. 37389

13. ABSTRACT

An investigation was conducted to determine the feasibility of extending the capability of ablation test facilities by surrounding the high enthalpy flow with a coaxial cold air jet. The investigation included both analytical and cold flow experimental studies. It was determined that the coaxial flow technique is extremely promising, offering the potential of easily doubling the facility model size capability. Results of the cold flow experimental tests and criteria for application of the technique to high enthalpy facilities are presented.

DD FORM 1 NOV 65 1473

UNCLASSIFIED

Security Classification

14. KEY WORDS	LINK A		LINK B		LINK C	
	ROLE	WT	ROLE	WT	ROLE	WT
ablation						
test facilities						
electric arc furnaces						
jet flow						
supersonic nozzles						